University of Alberta

A geochemical and Sm-Nd isotopic study of Cordilleran eclogites from the Yukon-Tanana terrane.

by

Jo-Anne Stafford Goodwin-Bell

A thesis submitted to the Faculty of Graduate Studies and Research in partial fulfillment of the requirements for the degree of Master of Science

Department of Earth and Atmospheric Sciences

Edmonton, Alberta

Spring, 1998

National Library of Canada
Acquisitions and Bibliographic Services
395 Wellington Street
Ottawa ON K1A 0N4
Canada

Bibliothèque nationale du Canada
Acquisitions et services bibliographiques
395, rue Wellington
Ottawa ON K1A 0N4
Canada

Your file Votre référence

Our file Notre référence

The author has granted a non-exclusive licence allowing the National Library of Canada to reproduce, loan, distribute or sell copies of this thesis in microform, paper or electronic formats.

L'auteur a accordé une licence non exclusive permettant à la Bibliothèque nationale du Canada de reproduire, prêter, distribuer ou vendre des copies de cette thèse sous la forme de microfiche/film, de reproduction sur papier ou sur format électronique.

The author retains ownership of the copyright in this thesis. Neither the thesis nor substantial extracts from it may be printed or otherwise reproduced without the author's permission.

L'auteur conserve la propriété du droit d'auteur qui protège cette thèse. Ni la thèse ni des extraits substantiels de celle-ci ne doivent être imprimés ou autrement reproduits sans son autorisation.

0-612-28939-7

Canada

University of Alberta

Faculty of Graduate Studies and Research

The undersigned certify that they have read, and recommend to the Faculty of Graduate Studies and Research for acceptance, a thesis entitled A geochemical and Sm-Nd isotopic study of Cordilleran eclogites from the Yukon-Tanana terrane submitted by Jo-Anne Stafford Goodwin-Bell in partial fulfillment of the requirements for the degree of Master of Science.

Dr. R. A. Creaser (co-supervisor)

Dr. P. Erdmer (co-supervisor)

Dr. J. P. Richards

Dr. R. G. Cavell

December 18, 1997

Abstract

Eclogites are found in a number of lenses within the Yukon-Tanana terrane, a large suspect terrane in the northern Cordillera. Samples collected from areas near Faro, Last Peak, Ross River, Simpson Range, and Stewart Lake were the focus of a geochemical and Sm-Nd isotopic investigation to determine the tectonic setting of the basaltic protoliths of the eclogites and the timing of high-pressure metamorphism.

The eclogites can be subdivided into four distinct groups on the basis of geochemical analysis. Eclogites from Faro, Ross River, Simpson Range and one from Stewart Lake are derived from n-MORB. Last Peak eclogites and one from Faro have within-plate basaltic protoliths. The remaining Stewart Lake eclogites are divided into 2 groups each with oceanic island-arc affinity; one with calc-alkaline basaltic-andesite characteristics and the other low-potassium tholeiitic characteristics. Sm-Nd dating of two eclogites resulted in ages of 281 ± 15 Ma (Faro) and 255 ± 8.1 Ma (Ross River). The results of this study have important implications for the various tectonic models proposed for the Yukon-Tanana terrane.

Acknowledgements

The author would like to thank her co-supervisors, Dr. R. A. Creaser and Dr P. Erdmer for their patient advice and assistance during the completion of this project. The author also appreciated the comments of examiners Dr. J. P. Richards and Dr. R. G. Cavell, whose thorough review of the manuscript resulted in many necessary improvements. The technical advice of Olga Levner and Steven Grant was invaluable during the completion of this project.

The author acknowledges funding, received by R. A. Creaser and P. Erdmer, from Lithoprobe in support of this project.

Finally, a large thank you to my husband and my parents for their unflagging belief that it would eventually "get done".

Table of Contents

	Page no.
Chapter 1 Introduction	
1.1 Introduction and Previous Work	1
1.2 Location	6
1.3 Purpose and Methods	6
1.4 Summary of Conclusions	8
Chapter 2 Regional Geology	
2.1 Tectonic Overview of the Canadian Cordillera	9
2.2 The Yukon-Tanana Terrane	
2.2.1 Terrane Nomenclature	12
2.2.2 Stratigraphy and Geology of the Yukon-Tanana Terrane	17
2.2.3 Models of the Tectonic Evolution of the Yukon-Tanana terrane	21
2.3 Relationships of the Yukon-Tanana Terrane to Surrounding Terranes and North America	
2.3.1 Slide Mountain and Cache Creek Terrane	31
2.3.2 Cassiar Terrane	34
2.3.3 Quesnellia Terrane	35
2.3.4 North America	35
2.4 Local Geology	36

Page no.

Chapter 3 Whole Rock Geochemistry

3.1 Introduction 40

3.2 Major Element Variations 44

3.3 Chemical Affinity and Tectonic Setting 53

3.4 Rare Earth Elements 65

3.5 Incompatible Elements 70

3.6 Conclusions 74

Chapter 4 Sm-Nd Systematics and Geochemistry

4.1 Introduction 75

4.2 Whole Rock Model Ages 75

4.3 Whole Rock Nd Geochemistry 79

4.4 Sm-Nd Geochronology 80

Chapter 5 Discussion and Conclusions

5.1 Summary of Results 90

5.2 Discussion

5.2.1 Geochemical and Age Correlations 91

5.2.2 Relationship to Slide Mountain 94

5.2.3 Constraints for Tectonic Models 99

5.3 Conclusions 107

page no.

References 110

Appendix 1: Analytical Methods 125

List of Tables

	Page no.
Table 1: Summary of terrane nomenclature	16
Table 2: Geochemical analysis results for whole rock samples	41
Table 3: Trace and rare earth elements for whole rock samples	42
Table 4: Trace and rare earth elements for mineral separates	43
Table 5: Summary of tectonic discrimination results	63
Table 6: Tectonic discrimnation ratios for whole rock samples	64
Table 7: Sm-Nd isotopic analysis results for Whole rock samples and mineral separates	86

List of Figures

Page no.

Chapter 1

1.1 Map of the Yukon-Tanana terrane with eclogite sample locations. 2

Chapter 2

2.1 Map of the Canadian Cordillera. 10

2.2 Map of the Yukon-Tanana terrane and surrounding terranes. 32

Chapter 3

3.1 Harker variation diagrams; A = TiO_2 versus SiO_2, B = P_2O_5 versus SiO_2. 45

3.2 Harker variation diagrams; A = FeO* versus SiO_2, B = MgO versus SiO_2. 47

3.3 Harker variation diagrams; A = MnO versus SiO_2, B = CaO versus SiO_2. 49

3.4 Harker variation diagrams; A = K_2O versus SiO_2, B = Na_2O versus SiO_2. 50

3.5 Harker variation diagram; Al_2O_3 versus SiO_2. 51

3.6 AFM diagram for Yukon-Tanana terrane eclogites. 52

3.7 Zr/TiO_2 versus Nb/Y for Yukon-Tanana terrane eclogites. 55

3.8 Ti-Zr-Y diagram for Yukon-Tanana terrane eclogites. 56

Page no.

3.9 Ti-Zr diagram for Yukon-Tanana terrane eclogites. 57

3.10 Ti-V diagram for Yukon-Tanana terrane eclogites. 59

3.11 Th/Yb-Ta/Yb diagram for Yukon-Tanana terrane eclogites. 61

3.12 Zr/Y-Zr diagram for Yukon-Tanana terrane eclogites. 62

3.13 REE diagrams; A = groups SLC and SLK, B = examples from the South Sandwich Islands and average MORB . 66

3.14 REE diagrams; A = group FRS, B = examples from the South Sandwich Islands and average MORB. 68

3.15 A = Incompatible element diagram for Last Peak and Faro (PE-80-F3) eclogites. B = REE diagram for Last Peak and Faro (PE-80-F3) eclogites. 69

3.16 Incompatible element diagrams; A = groups SLC and SLK, B = examples from the South Sandwich Islands. 71

3.17 Incompatible element diagrams; A = group FRS, B = examples from the South Sandwich Islands. 73

Chapter 4

4.1 Plot of $\varepsilon\,^{143}Nd$ versus time for selected eclogites and depleted mantle. 78

4.2 A = Ti versus $\varepsilon\,^{143}Nd_{metamorphism}$ for Yukon-Tanana terrane eclogites. B = Zr versus $\varepsilon\,^{143}Nd_{metamorphism}$ for Yukon-Tanana terrane eclogites. 81

4.3 A = V versus $\varepsilon\,^{143}Nd_{metamorphism}$ for Yukon-Tanana terrane eclogites. B = Nb versus $\varepsilon\,^{143}Nd_{metamorphism}$ for Yukon-Tanana terrane eclogites. 82

4.4 Sm-Nd isochron diagram for Faro eclogite PE-80-F1. 87

Page no.

4.5 Sm-Nd isochron diagram for Ross River eclogite PE-85-21. 88

Chapter 5

5.1 REE diagram for selected Yukon-Tanana terrane eclogites and Slide Mountain terrane metabasalts 96

5.2 Incompatible element diagram for selected Yukon-Tanana terrane eclogites and Slide Mountain terrane metabasalts. 98

5.3 Model of the evolution of the Nisutlin assemblage Mississippian to Triassic 104

5.4 Model of the evolution of the Nisutlin/Anvil block at ~ 360 Ma. 106

List of Abbreviations

YTT = Yukon-Tanana terrane.

TTZ = Teslin Tectonic zone.

FRS = group of eclogite samples from Faro, Ross River, Simpson Range, and one from Stewart Lake with normal mid-ocean ridge basalt affinity.

SLC = group of eclogite samples from Stewart Lake with calc-alkaline basaltic andesite affinity.

SLK = group of eclogite samples from Stewart Lake with low-potassium tholeiitic basalt affinity.

BSR = group of eclogite samples from Last Peak and one from Faro with continental within-plate affinity.

MORB = normal mid-ocean ridge basalt.

OFB = ocean floor basalt.

CAB = calc-alkaline basalt.

LKT = low-potassium tholeiitic basalt.

WPT = within-plate basalt either continental or oceanic.

REE = rare earth elements; prefix **L** = light and prefix **H** = heavy

LILE = large ion lithophile element

Ma = unit in millions of years

Ga = unit in billions of years

Chapter 1 Introduction

1.1 Introduction and Previous Work

The Yukon-Tanana terrane is a large and enigmatic terrane in the northern Cordillera between autochthonous North American crust to the east and suspect terranes to the west (Mortensen, 1992). The terrane has been divided into three allochthonous assemblages (Tempelman-Kluit, 1979), the Nisutlin, Anvil and Simpson assemblages. Eclogites occur in many locations within the Nisutlin and Anvil assemblages (figure 1.1). They are typically well-preserved, although some have undergone retrograde metamorphism (Erdmer and Helmstaedt, 1983; Erdmer 1987, 1991). The eclogites represent the most conclusive evidence of primarily Paleozoic subduction within the northern Cordillera and provide unambiguous temperature, pressure and time markers in the pre-accretion history of the Yukon-Tanana terrane (Creaser et al., 1997a).

Numerous tectonic models have been developed and refined to explain the origin and evolution of the Yukon-Tanana terrane (YTT). The first model, proposed by Tempelman-Kluit (1979), interpreted the Teslin Tectonic zone as part of a subduction

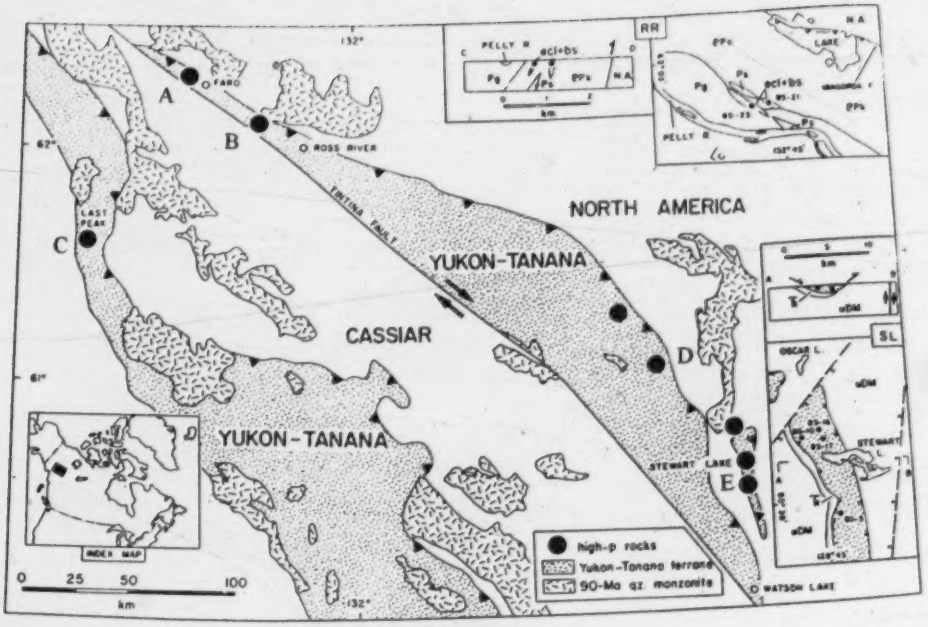

Figure 1.1. Map of the Yukon-Tanana terrane displaying eclogite sample locations (A-E); teeth symbols in upper plate rocks. Eclogite and blueschist occur northwest of Ross River (B); eclogite occurs in the other localities. Location A = Faro; B = Ross River; C = Last Peak; D = Simpson Range; E = Stewart Lake. Samples at A = PE-80-F1, PE-80-F2, PE-80-F3; at B = PE-80-19, PE-80-21; at C = PE-80-BSR, PE-80-BSRC; at D = CRE-95-205; at E = PE-85-10, PE-85-10B, PE-85-11-1, PE-85-11-2, PE-85-12, PE-85-16B, PE-85-17, PE-85-18, PE-85-18B. Inset "SL": map and idealized cross section of Stewart Lake; Tr = Triassic North American strata, uDM = Devono-Mississippian North American strata. Inset "RR" map and idealized cross section of Ross River; NA = rocks of North American affinity, ecl + bs = eclogite and blueschist, Ps = serpentinite, PPk = mylonitic muscovite-quartz schist and quartzite, Pg = greenstone. (From Erdmer, 1987.)

zone complex which preserved trench mélange, ophiolite sequences and the plutonic roots of a volcanic arc. The presence of eclogitic rocks strongly supported this argument and subduction zone processes were emphasized by Hansen (1987, 1989, 1992a and 1992b) and Hansen et al. (1989, 1991). Mortensen and Jilson (1985) and Mortensen (1992) proposed an alternative model in which the terrane evolved as a package with coherent internal stratigraphy in a subduction system. Although high-pressure metamorphism prior to the Mesozoic accretion of the YTT to the North American continental margin has long been recognized as a key event in the various tectonic models proposed, the exact timing and duration of the subduction events are poorly defined, and it has not yet been determined whether the eclogites are the product of one or several periods of subduction (Creaser et al., 1997a).

Previous work on the YTT consists mainly of structural examination of various sections of the terrane and the Teslin tectonic zone (TTZ) in particular (Mortensen and Jilson, 1985; Hansen 1987, 1989, 1992a and 1992b; Hansen et al., 1989, 1991). Some age dating of plutons and gneisses has been performed (Mortensen, 1992). Study of the eclogites within the YTT focused on determination of the temperature and pressure conditions of the high-pressure metamorphism (Erdmer and Helmstaedt, 1979; Erdmer

1987, 1991) and K-Ar and $^{40}Ar/^{39}Ar$ mica cooling ages (Erdmer and Armstrong, 1988; Erdmer et al., 1996, 1997) to provide minimum estimates of the timing of subduction events. Detailed geochemical study of the eclogites had not been previously undertaken and determination of the actual age of high-pressure metamorphism is limited to two U-Pb zircon ages (Creaser et al., 1997a; K. Fallas, 1997, personal communication).

The focus of this research on the eclogites is two-fold. Previous tectonic models were based on the assumption that the eclogites are geochemically and tectonically equivalent to each other. Therefore, the first objective was to characterize the basaltic protoliths of the eclogites and determine their tectonic setting using whole rock geochemical analysis of major, trace and rare earth elements. Rare earth elements and some trace elements are generally considered to be immobile during low-grade to high-grade metamorphism (Vidal and Hunziker, 1985) and are useful in determining the tectonic setting of basaltic and gabbroic protoliths. The depositional setting of the basaltic protoliths is very important to understanding the origin of the eclogites and their role in the overall tectonic evolution of the YTT

The second objective of this research was to determine the age of high -pressure metamorphism using the Sm-Nd isotope system. Both the K-Ar and Rb-Sr isotope

systems have been applied to the dating of blueschist and eclogite as detailed by Vidal and Hunziker (1985). K-Ar dating, typically applied to micas, yields cooling ages and minimum estimates for the timing of high-pressure metamorphism. Rb-Sr ratios are usually low in mafic and ultramafic rocks. Rb mobility during metamorphism limits the application of the Rb-Sr system to widespread dating of eclogites. The U-Pb zircon and Sm-Nd whole-rock-garnet-pyroxene methods have proven more reliable in dating of eclogites (Griffin and Brueckner, 1980; Sanders et al., 1984; Mørk and Mearns, 1986; Mørk et al., 1988; Paquette et al., 1989; Thöni and Jagoutz, 1992; Miller and Thöni, 1995). The garnet-pyroxene pair is considered very favourable for Sm-Nd dating as the two minerals fractionate Sm and Nd more efficiently than most rock-forming minerals (Griffin and Brueckner, 1980) and have high blocking temperatures for Sm-Nd diffusion (Mørk et al., 1988). Sm and Nd are nearly identical in their chemical behaviour and because rare earth elements are immobile during metamorphism (Griffin and Brueckner, 1980) assuming total recrystallization has not occurred during retrograde events. The Sm-Nd isotope system is useful in determining the actual age of crystallization of the garnet and pyroxene minerals and therefore, the age of high-pressure metamorphism.

The results from the geochemical and Sm-Nd isotope study of the Yukon-Tanana eclogites answer important questions concerning the tectonic development of the eclogites and the YTT as a whole. Existing tectonic models are examined below in light of the new data obtained on the YTT.

1.2 Location

The eclogites studied are found in several lenses in the central Yukon (refer to figure 1.1). They occur over a strike length of several hundred kilometres between the Tintina Fault and the Teslin Tectonic zone (Erdmer, 1987 and 1992). Samples for this study were collected from Faro, Last Peak, Ross River, Stewart Lake and Simpson Range by P. Erdmer and R.A. Creaser.

1.3 Purpose and Methods

The following methods were employed to fulfil the research objectives of this study of eclogites from the YTT:

(1) Characterization of the basaltic protolith(s) of the eclogites using whole rock major, trace and rare earth element geochemistry from seventeen samples.

(2) Determination of the tectonic setting(s) of the basaltic protolith(s) of the eclogites using tectonic discrimination, multielement and spider diagrams involving trace and rare earth elements.

(3) Determination of the age of high-pressure metamorphism and characterization of the basaltic protolith(s) in the YTT using the Sm-Nd system on whole rock samples and garnet and pyroxene separates. seventeen isotopic analyses are presented for whole rock samples and mineral separates.

(4) Comparison of the resulting dates with those obtained using U-Pb zircon and $^{40}Ar/^{39}Ar$ mica techniques.

(5) Comparison of the results with data found in current literature to aid in interpretation and evaluation of the geological development of the eclogites.

1.5 Summary of Conclusions

In this thesis it is shown that the eclogites of the YTT evolved from basaltic protoliths originating in very different tectonic settings. Eclogites from Faro, Ross River, Simpson Range and one sample from Stewart Lake have normal mid-ocean ridge basaltic (MORB) protoliths and are labeled as group FRS. Other Stewart Lake eclogites share oceanic island-arc affinity and can be further subdivided into two groups. One group SLC displays calc-alkaline basaltic-andesite character (higher silica) and the other group SLK displays low-potassium tholeiitic character. Continental within-plate basaltic character is displayed by eclogites from Last Peak and one from Faro labeled group BSR. Based on the results of the geochemical analysis of the eclogites, the correlation of all mafic igneous rocks in the YTT with Slide Mountain terrane should be revised.

The Sm-Nd dates obtai ned for two eclogites in this study are broadly consistent with the ages obtained by other workers using both $^{40}Ar/^{39}Ar$ mica and U-Pb zircon techniques. Eclogites from Stewart Lake and Simpson Range are older than those at Faro, Ross River and Last Peak. The results support a conclusion that at least two phases of subduction are recorded by rocks in the YTT.

Chapter 2 Regional and Local Geology

2.1 Tectonic Overview of the Canadian Cordillera

The geological architecture of the Canadian Cordillera is the product of an evolution that spans more than 1.6 Ga and which involved a variety of tectonic processes acting upon and adjacent to the ancient continental margin of North America (Gabrielse and Yorath, 1991). The main elements of metamorphism, plutonism, volcanism and structure are dominantly the result of Mesozoic to Cenozoic tectonism. Five geological and physiographic belts reflect the result of these processes. From east to west they comprise the Foreland, Omineca, Intermontane, Coast, and Insular belts, each of which is defined by a combination of lithological, structural, tectonic and physiographic characteristics (figure 2.1). The five belts form the continental crust of the Cordillera which is about 45 to 50 km thick beneath the Foreland belt, 30 km under the Omineca, Intermontane, and Coast belts and underneath the Insular belt, thins from nearly 30 km in the east to less than 3 km at the edge of the continental slope (Gabrielse et al., 1991).

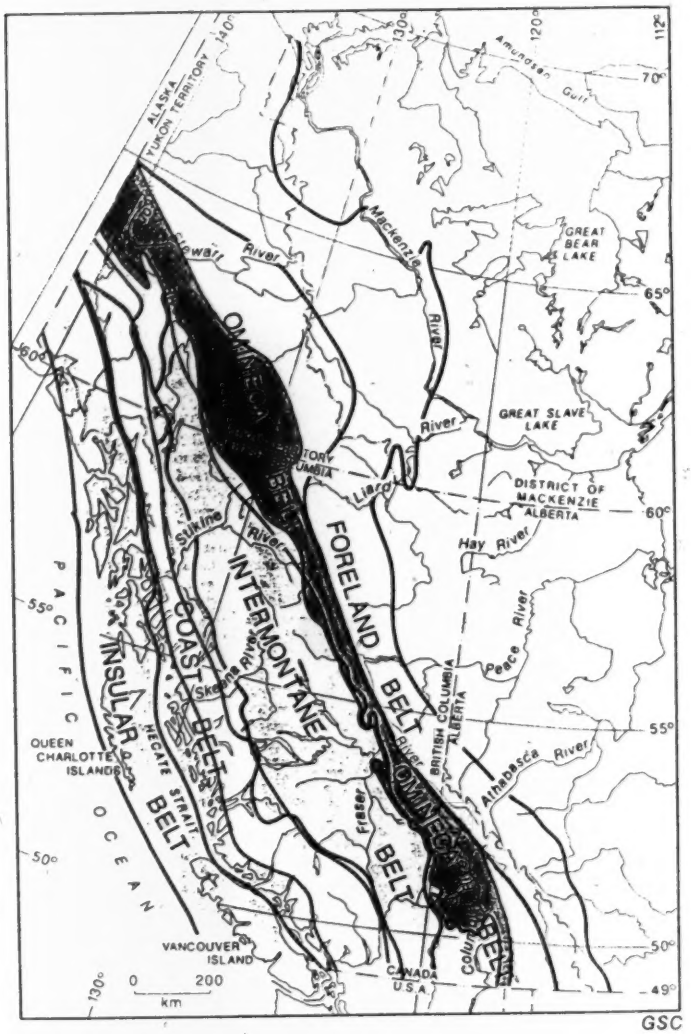

Figure 2.1. Map of the Canadian Cordillera showing a comparison of the distribution of the five morphogeological belts with the pericratonic and displaced terranes and accreted terranes. (From Gabrielse et al., 1991.)

Accreted pericratonic and suspect terranes ma ke up over 70% of the North American Cordillera (Coney et al., 1980). West of the Foreland belt, the Omineca Belt is comprised largely of pericratonic terranes and the remaining three belts consist of allochthonous terranes. The allochthonous terranes are characterized by tectonic, structural and stratigraphic styles unlike those of the North American continental margin (Coney et al., 1980). Some terranes display paleomagnetic evidence that suggests large latitudinal displacements and others contain distinctive exotic faunas.

Parts of the Canadian Cordillera can be compared to modern ocean tectonic settings and to other orogenic belts (Gabrielse and Yorath, 1991). The tectonic settings of Stikinia terrane and Quesnellia terrane can be equated with the modern Japanese Archipelago. Wrangellia terrane, which originated as a rifted arc, resembles the Lau Basin behind the Tonga Trench. The Coast Plutonic Complex has been compared with the Andean margin but is much more complicated. Overall, the Cordillera has been compared to the Himalayas (Coney et al., 1980) and the Alps (Gabrielse and Yorath, 1991) but it is characterised by more plutonic rocks and obducted oceanic crust and does not represent a continent-continent collision. The Cordillera incorporates characteristics of the various types of margin settings but has experienced a more complex geological history.

2.2 The Yukon-Tanana Terrane

2.2.1 Terrane Nomenclature

Terrane terminology in the Northern Cordillera and the YTT, in particular, varies considerably between authors. This is a summary of the various terrane names used for the YTT.

In central and western Yukon, metamorphosed rocks between the Denali and Tintina Fault zones were originally assigned to the Yukon Group by Cairnes (1914). Tempelman-Kluit (1976) renamed these rocks the Yukon Crystalline Terrane.

Subsequent field work (Tempelman-Kluit, 1979) led to the subdivision of the terrane into two distinct parts. The northwest was termed the Yukon Cataclastic Complex and was further subdivided into three assemblages. The Nisutlin Allochthon is composed of protoclastic, weakly metamorphosed, sedimentary and volcanic rocks to mylonite, ultramylonite, blastomylonite and schist, at the lowest structural level. The second sheet is the Anvil Allochthon, a sheared ophiolite and the highest sheet, the Simpson Allochthon contains various cataclastic granitic rocks. The southern portion was called the Teslin Suture Zone (Tempelman-Kluit, 1979), now termed the Teslin

tectonic zone (TTZ), a zone of steeply dipping cataclastic rocks at least 15 km wide. Rocks correlated with the three allochthonous assemblages occupy this zone (Tempelman-Kluit, 1979).

Coney et al. (1980) and most subsequent workers included the Yukon Cataclastic Complex within the YTT as recognized in Alaska (Mortensen, 1992). The remaining portion of the terrane was renamed the Tracy Arm terrane (Coney et al., 1980). This terrane was renamed the Nisling terrane (Wheeler and McFeely, 1987; Wheeler et al., 1988). The Nisling terrane is divisible in two assemblages; the Nisling Assemblage, a metamorphosed passive continental margin sequence of Upper Proterozoic to Lower Cambrian age and the Nasina Assemblage, Cambrian to Devonian, partly metamorphosed carbonaceous and siliceous offshore sediments. Mortensen and Jilson (1985) stated that the YTT resembles the Kootenay terrane of British Columbia in its plutonic and tectonic history, stratigraphic sequence and ambiguous relationship with the continental margin and therefore may be a displaced part of the Kootenay terrane. Later compilations by Wheeler et al. (1988) and Wheeler and McFeely (1991) correlated part of the YTT with the Nisling terrane and the remainder with the Nisutlin subterrane of the Kootenay terrane

of British Columbia. East of the Teslin tectonic zone, in southern Yukon, part of the YTT was named the Dorsey terrane (Wheeler et al., 1988).

Hansen (1990) redefined the YTT and divided it into the Nisling and Teslin-Taylor Mountain terranes on the basis of metamorphic cooling ages and apparent structural level. The Nisling terrane yielded Early Cretaceous cooling ages and occurs at low structural levels, and the Teslin-Taylor Mountain occurs at high structural levels, with pre-Late Jurassic cooling ages. Hansen (1990) assigned the augen orthogneiss suite of Mortensen and Jilson (1985) to the Nisling terrane and the Nisutlin and Anvil Allochthons (Tempelman-Kluit, 1979), consisting of metasedimentary and metavolcanic tectonites with rare eclogites and blueschists are assigned to the Teslin-Taylor Mountain terrane.

Erdmer (1992) described the Yukon-Tanana terrane as including a high pressure/ high temperature component, namely the three allochthonous assemblages of Tempelman-Kluit (1979) and a suite of Devonian-Mississippian peraluminous orthogneisses. The two parts preserve different metamorphic, structural and kinematic histories (Hansen, 1990, 1992b).

Stevens et al. (1996) retained the usage of Nisutlin and Anvil Allochthons as lithotectonic assemblages, but not the Simpson Allochthon for the YTT. These authors found no direct evidence to support the assignment of the Nisutlin and Anvil Allochthons to separate terranes, as rocks in both assemblages have the same metamorphic and structural characteristics. Stevens et al. (1996) correlated the Nisutlin assemblage with the middle unit of Mortensen (1992). Rocks of the Anvil assemblage may also correlate with this middle unit. If these authors are correct, it implies that the Nisutlin and Anvil assemblages interfinger and may be depositionally related (Stevens et al., 1996).

Stevens et al. (1996) also suggested that graphitic phyllite in the TTZ, assigned to the Cassiar terrane by Hansen et al. (1991), is in depositional contact with rocks of the Yukon-Tanana terrane. Creaser et al. (1997b) showed, on the basis of Nd isotopes, that this unit cannot be miogeoclinal (e.g. Cassiar). Early Mississippian hornblende-bearing metaplutonic rocks assigned to the Teslin-Taylor Mountain terrane by Hansen et al. (1991) are included in the Nisutlin assemblage by Stevens et al. (1996), based on igneous contacts with metasedimentary rocks of the Yukon-Tanana terrane. A summary of terrane nomenclature is listed in table 1.

Table 1

Terrane Nomenclature ~ summary of the various names used for the YTT

Cairnes (1914) ~ Yukon Group

Tempelman-Kluit (1976) ~ Yukon Crystalline terrane

Tempelman-Kluit (1979) ~ Yukon Cataclasitic Complex and Teslin Suture Zone
Yukon Cataclastic Complex = Nisutlin, Anvil and Simpson Allochthons

Coney et al. (1980) ~ Yukon Cataclastic Complex = Yukon-Tanana terrane + Tracey Arm terrane
Wheeler and McFeely (1987) and Wheeler et al. (1988) ~ Tracey Arm terrane = Nisling Assemblage

Mortensen and Jilson (1985) ~ Yukon-Tanana terrane = Kootenay terrane

Wheeler et al (1988) and Wheeler and McFeely (1991) ~ Part of YTT = Nisling terrane, part = Nisutlin subterrane of Kootenay terrane, and part = Dorsey terrane

Hansen (1990) ~ YTT = Nisling and Teslin-Taylor Mountain terranes

Stevens et al. (1996) ~ YTT = Nisutlin and Anvil Allochthons

2.2.2 Stratigraphy and Geology of the Yukon-Tanana Terrane

The oldest preserved rocks of the YTT are pre-Devonian quartzofeldspathic metasedimentary rocks with some pelitic schist and marble, locally overlain by Late Devonian to mid-Mississippian metavolcanic rocks and intruded by granitic plutons of the same age (Mortensen, 1992). The depositional age of these rocks is poorly constrained. These metasedimentary rocks have been interpreted as a passive margin sequence (Mortensen, 1992).

Carbonaceous fine-grained quartz sandstone, siltstone and pelite with minor marble and rare pebble conglomerate were deposited from mid-Devonian to mid-Mississippian time. The date is constrained by both fossil evidence and Pb model ages (Mortensen, 1992).

Voluminous and widespread magmatism began in the Late Devonian (Mor tensen, 1992), mafic and felsic metavolcanic rocks from a submarine environment being interlayered with metasedimentary rocks (Mortensen and Jilson, 1985). U-Pb zircon dates range from the Late Devonian to Early Mississippian (Mortensen, 1992).

Two large plutonic suites of this same age are also dominant in the YTT. The first plutonic suite is mainly felsic, peraluminous and moderately to strongly foliated with a large inherited zircon component. It occurs in both the western and southwestern Yukon and the TTZ (Mortensen, 1992). The second plutonic suite is composed of hornblende-bearing, metaluminous, massive to strongly deformed and metamorphosed diorite to monzonite with minor gabbro (Mortensen, 1992). Both the metavolcanic and metaplutonic rocks of Late Devonian to mid-Mississippian age represent the products of continental arc magmatism (Mortensen, 1992; Grant, 1997).

Within the YTT, the period between mid-Mississippian to late Early Permian time is marked by either non-deposition or rocks deposited during this interval have been eroded (Mortensen, 1992).

A second phase of magmatism in the YTT is mid-Permian in age and resulted in the emplacement of felsic metaplutonic and minor metavolcanic rocks (Mortensen, 1992). Mid- to Late Permian metamorphic cooling ages have been obtained for high-pressure metamorphic rocks in the Faro and Ross River areas (Wanless et al., 1978; Erdmer and Armstrong, 1988). These rocks lay northeast of the Permian metaigneous suites prior to Late Cretaceous-early Tertiary offset on the Tintina Fault. The presence of blueschist

and eclogite facies rocks indicates that metamorphism occurred in a subduction zone (Tempelman-Kluit, 1979; Erdmer and Helmstaedt, 1983; Erdmer, 1987).

The major ductile deformation in YTT rocks (D1) appears to have occurred between the Late Permian and the onset of renewed magmatism in Late Triassic time (Mortensen, 1992). The D1 fabrics developed in mid-Permian metaigneous rocks which are crosscut by undeformed plutons of latest Triassic age (Mortensen, 1992). D1 is a pervasive, subhorizontal to shallowly dipping foliation which also involves mylonitic textures and a pronounced stretching lineation (Erdmer, 1985; Mortensen and Jilson, 1985). It was accompanied by middle greenschist to middle amphibolite facies metamorphism. The nature of the D1 deformation is unknown. Tempelman-Kluit (1979) attributed the fabric to deformation in a subduction zone. Hansen (1989, 1990) suggests regional extension may be involved in the deformation and Mortensen (1992) supports a continent-continent collision model.

A second, less intense phase of deformation, D2, is also recorded in rocks in the YTT. It is associated with metamorphism of at least middle greenschist facies. It produced outcrop-scale folds with a strong crenulation cleavage (Erdmer, 1985; Mortensen and Jilson, 1985). Hansen (1988) suggests the ductile structures preserved

within the TTZ record progressive evolution from a dominantly convergent margin (D1) to an oblique margin with right-lateral strike-slip translation (D2).

Plutonic activity began again in the Late Triassic and continued until the Middle Jurassic resulting in massive, undeformed and strongly differentiated plutons, some of which contain inherited zircons (Mortensen, 1992). Similar plutons are found in other terranes and this suite may be a "pinning" assemblage between the YTT and the Stikine terrane, Nisling terrane, Dorsey terrane and possibly Cache Creek terrane (Mortensen, 1992).

Weakly deformed and metamorphosed ar gillite, argillaceous limestone, sandstone and minor conglomerate of Upper Triassic age occur in several areas of the YTT (Mortensen, 1992). These sedimentary rocks are in close contact with ultramafics and greenstones of the Slide Mountain terrane and due to the faulted contacts between the Yukon-Tanana and Slide Mountain terranes, it is unclear whether these rocks are related to the YTT or the Slide Mountain terrane (Mortensen, 1992).

The YTT was extensively imbricated by regional scale thrust faults. Six major thrust have been identified (Mortensen and Jilson, 1985). These faults are typically

parallel or at a low angle to the cataclastic foliation (Erdmer, 1985). They postdate deposition of fossiliferous Late Triassic sedimentary rocks, but are crosscut by mid-Cretaceous plutons (Mortensen and Jilson, 1985).

2.2.3 Models of the Tectonic Evolution of the Yukon-Tanana Terrane

Tempelman-Kluit (1979) proposed a two-stage plate-tectonic model for the formation and emplacement of the Yukon-Tanana terrane. He concluded that the TTZ was a subduction complex, formed at an arc-ocean boundary in the Late Triassic-Early Jurassic, that evolved into an arc-continent collision following the subduction of the Anvil Ocean. The arc developed above a southwestward-dipping subduction zone on the continental margin of Stikinia and the cataclastic rocks of the TTZ and the allochthons are a structural mélange. The rocks of the Nisutlin Allochthon presumably were trench and forearc sediments sheared during subduction and imbricated with slabs of oceanic crust of the Anvil Allochthon and with the plutonic roots of the island arc, the Simpson Allochthon. The presence of eclogite supports the interpretation of these rocks as mélange related to subduction (Tempelman-Kluit, 1979). The second stage of the model

involved the obduction of the arc complex onto the North American craton. Thrusts transported cataclastic sheets imbricated with slices of North American strata more than 100 km northeastward of the suture.

Tempelma n-Kluit (1979) proposed a consistent order of superposition of the allochthons within the transported sheets. The Simpson Allochthon rests on the Anvil Allochthon and the Anvil Allochthon overlies the Nisutlin Allochthon. He also indicated that depositional relationships between the assemblages were unknown and no internal stratigraphy was recognizable.

Erdmer (1985) concluded that the stacking order of the allochthons was much more complex than previously thought by Tempelman-Kluit (1979). He also suggested that the observation of less deformed autochthonous rocks overlying cataclastic rocks indicates the development of horses or duplexes along the major thrust faults within the YTT. Erdmer (1985) agreed that collision of an arc with the passive western North American margin , proposed by Tempelman-Kluit (1979), is the simplest explanation for the proposed shearing and flattening within the TTZ and the complex stacking of the allochthons. The analysis of the eclogite also constrains the conditions of deformation for

the eclogite and the host structural mélange to pressures above 12 MPa and temperatures greater than 650-700°C (Erdmer, 1985).

Mortensen and Jilson (1985) proposed a model for the evolution of YTT which was refined by Mortensen (1992). The terrane is interpreted to be the product of episodic mid-Paleozoic to early Mesozoic continental arc magmatism. This composite rests on pre-Devonian passive continental margin deposits underlain by probable continental crust (Mortensen and Jilson, 1985; Mortensen, 1992). Mortensen (1992) attributes both the Late Devonian to mid-Mississippian igneous suite and the mid-Permian igneous suite, associated with blueschists and eclogites, to continental arc magmatism. The collision of the YTT with another continental mass (possibly North America) could be responsible for the D1 fabrics and its associated metamorphism (Mortensen and Jilson, 1985; Mortensen, 1992), now known to be older. The assemblage was then actively eroded and immature clastic sediments were deposited on it. Thrust faulting which accompanied and or followed Triassic-Jurassic plutonism may represent the final stages of the amalgamation of the Intermontane Superterrane (Mortensen, 1992). By mid-Cretaceous the layered metamorphic sequence and the Late Triassic clastic rocks

derived from it were imbricated with middle and upper Paleozoic ophiolites (Mortensen and Jilson, 1985).

Hansen (1988, 1989) proposed a model for the tectonic evolution of the YTT broadly similar to Tempelman-Kluit's (1979) but with modifications based on structural and geochronological evidence. Tempelman-Kluit (1979) proposed a west-dipping subduction environment in which Stikine terrane represented the magmatic arc and the YTT was entirely composed of trench mélange. Hansen (1988) suggests that at least a some of the YTT represents the arc and argues that the Yukon-Tanana and Slide Mountain terranes evolved as parts of the same convergent margin complex, based on their similarities in a regional tectonic context.

The YTT represents preserved components of a magmatic arc and remnants of the deep portion of an ancient west-dipping subduction complex (Hansen 1988, 1989). The imbricated accretionary complex and higher crustal levels of the arc are preserved within the Slide Mountain terrane. The TTZ represents material from the accretionary prism underplated to the arc hanging-wall during subduction.

In this model, the Yukon-Tanana and Slide Mountain terranes (arc and accretionary complex) together form a composite terrane and comprise the overriding

plate and the hanging-wall block (Hansen 1988). The subducting oceanic crust (Anvil Ocean) and adjoining continental lithosphere (North American continental margin) form the descending plate and the footwall block. The TTZ forms part of the décollement between the two converging plates and structural and kinematic relations documented within this zone record the interaction of the magmatic arc accretionary assemblages in the upper plate with the descending plate (Hansen, 1988).

B-type subduction, in which oceanic lithosphere is subducted (Hansen, 1992a and b) began in the Permian and, because convergence was oblique (Hansen 1988, 1989), subduction related strike-slip faults were initiated within the accretionary complex on the leading edge of the hanging-wall plate. Hansen (1988) indicates that these faults formed at a high angle near the surface and shallowed at depth into the plate décollement and developed progressively arcward as oblique subduction continued. Displacement along these faults led to the formation of tectonic slivers distributed laterally parallel to the margin (Hansen, 1988, 1989). Hansen (1988) suggests that this model predicts the present distribution of the Yukon-Tanana and Slide Mountain terranes within the Cordillera.

Subsequent to the final accretion, in Early Jurassic time, of the laterally displaced Yukon-Tanana/Slide Mountain composite terrane, the terrane was tectonically imbricated and transported onto North America as the result of a reversal in subduction polarity and a change to A-type subduction, in which continental lithosphere is subducted (leading edge of North America; Hansen, 1992a and b) and continued convergence from the west (Hansen 1988, 1989, 1990). As a result of the overthrusting North American strata were tectonically buried. This overthickened crust underwent gravitational collapse and crustal extension in the mid-Cretaceous (Hansen 1989, 1990) resulting in tectonic unroofing and exposure of North American crust. Hansen (1989) suggests that the peraluminous orthogneiss bodies and associated metasedimentary rocks within the YTT may be autochthonous North American crust.

The occurrence of eclogite facies rocks is commonly the only evidence that a metamorphic belt underwent high pressure conditions. Eclogitic rocks within the St. Cyr klippe provide a lithologic link between the TTZ and a local nappe in the YTT (Erdmer, 1992). This supports a structural unity between the Nisutlin, Anvil and Simpson Allochthons and the TTZ (Erdmer, 1992).

The presence of eclogite has a bearing on the terrane affinity of the Anvil allochthon, previously correlated with the Slide Mountain terrane (Wheeler et al., 1991), and the Teslin-Taylor Mountain terrane (Hansen, 1990). Hansen et al. (1991) considered the Anvil Allochthon, Slide Mountain and Teslin-Taylor terranes as parts of a single lithotectonic assemblage that experienced different metamorphic histories directly related to their depths within the subduction zone. The Slide Mountain terrane represents the relatively unmetamorphosed accretionary prism and the Teslin-Taylor Mountain terrane records high P/T metamorphism, experienced at deep levels within the subduction zone (Erdmer, 1992). The Anvil Allochthon falls between these two end members (Erdmer, 1992). Based on evidence from the St. Cyr klippe (Erdmer, 1992), it appears that whole ophiolitic slices were subducted and transferred to the overriding plate as suggested in the model of Hansen (1989, 1992a and b).

A U-Pb zircon date (Creaser et al., 1997a) of 269 ± 2 Ma for a Last Peak eclogite, in the TTZ, combined with $^{40}Ar/^{39}Ar$ mica cooling dates from Yukon-Tanana eclogites and blueschists (Erdmer et al., in press) of 260-270 Ma provides a geochronologic "pin" in the evolution of the terrane. It also shows that high-pressure metamorphism was a relatively short lived event. Tectonic events in the 260-270 Ma period may be

responsible for the D1 fabrics in many YTT rocks (Creaser et al., 1997a). A separate regional tectono-magmatic event associated with calc-alkaline magmatism occurred in the Late Triassic to Early Jurassic in the YTT and in accreted terranes to the west and may be related to final assembly of the Intermontane Belt (Mortensen, 1992). This information requires a revision of models that assume continued subduction through Late Triassic or Early Jurassic (Tempelman-Kluit, 1979; Hansen, 1992a and b).

Erdmer et al. (in press) reported that eclogite and blueschist rocks from Yukon and Alaska that occur as primary units in or tectonically interleaved with the Yukon-Tanana and Slide Mountain terranes preserve a partial record of Middle Paleozoic, Late Paleozoic and Early Mesozoic subduction and subsequent unroofing. Analysis of eclogites near Faro, Ross River, Last Peak, Stewart Lake, and in the St. Cyr Klippe indicate the rocks were metamorphosed at depths ≥ 40 km, characteristic of type C eclogites. In some localities, eclogite metamorphism was predated by blueschist facies metamorphism and final cooling. The authors proposed that either episodic accretion of short-lived separate arcs or protracted convergence at a single subduction zone is a characteristic mechanism of crustal growth in the northern Cordillera.

Other workers have proposed alternative theories for the evolution of the YTT. Primary contact relationships and intrusive contacts indicate that part of the Nisutlin assemblage has a pre-Early Mississippian depositional age and that the rocks may have formed in a regionally extensive continental crustal terrane (Mortensen and Jilson, 1985; Stevens, 1994; Stevens et al., 1996). This would suggest that the Nisutlin Allochthon cannot have formed as a Late Paleozoic-Early Mesozoic subduction zone mélange.

Stevens et al. (1996) suggested that the Nisutlin assemblage was part of a crustal block that lay outboard of the North American continental margin in Mississippian time and that it lay in the hanging-wall plate of a Permo-Triassic subduction zone as a relatively coherent assemblage. In west-central Yukon, Permian calc-alkaline igneous rocks have continental magmatic-arc affinities and may represent part of an arc formed on the Nisutlin assemblage (Stevens et al., 1996). The authors also indicate that uplift of the eclogite and blueschist and the latest penetrative deformation of the Nisutlin assemblage occurred after subduction of the Slide Mountain Ocean, during Late Triassic to Early Jurassic collision of the YTT with North America.

Creaser et al. (1997b) interpreted the paleoenvironment for the Nisutlin assemblage to be at the outermost margin of the North American continent, in an area that

received detritus from both the North American craton in the early Paleozoic and a juvenile magmatic arc source. These authors also indicated that the geochemistry of the Anvil greenstones does not support correlation with Slide Mountain greenstones as previous tectonic models have suggested.

Stevens (1994) proposed an alternative model in which the TTZ represents a doubly vergent transpressive shear zone with characteristics of the lower portion of a flower structure. Brown et al. (1995) concluded that the TTZ does not display deformation characteristic of a subduction mélange. A coherent stratigraphy is preserved in metasedimentary rocks despite intense deformation (Stevens, 1994; Brown et al., 1995; Stevens et al., 1996), which in agreement with the findings of Mortensen and Jilson (1985).

Stevens and Erdmer (1996) stated that structural characteristics of the TTZ are best modelled by oblique eastward and upward movement of rocks over a detachment. This movement may have coincided with the top of thinned North American crust, producing easterly vergent shear and localized or widespread tectonic wedging and back thrusting producing westerly vergent shear. The transpressive deformation postdates formation of the Nisutlin assemblage and subduction of the Slide Mountain Ocean floor

(Stevens and Erdmer, 1996). The authors indicate that the western margin was truncated by Cretaceous strike-slip faults and transported northward, as suggested by Hansen (1988, 1989). The peraluminous orthogneiss acted as a tectonic wedge (Stevens and Erdmer, 1996) and was over thrust by the Nisutlin and Anvil assemblages in Early Jurassic and were unroofed by local extension in the Cretaceous (Stevens and Erdmer, 1996; Hansen, 1989).

2.3 Relationships of the Yukon-Tanana Terrane to Surrounding Terranes and North America

2.3.1 Slide Mountain and Cache Creek

The Slide Mountain and Cache Creek terranes of the Canadian Cordillera repre sent the remains of two Paleozoic ocean basins (Smith and Lambert, 1995). Lithological differences between the two terranes have long been recognized. Slide Mountain terrane is the easternmost allochthonous terrane (figure 2.2) and it occurs as klippen resting on the YTT and autochthonous North American miogeoclinal strata, and as thrust bounded

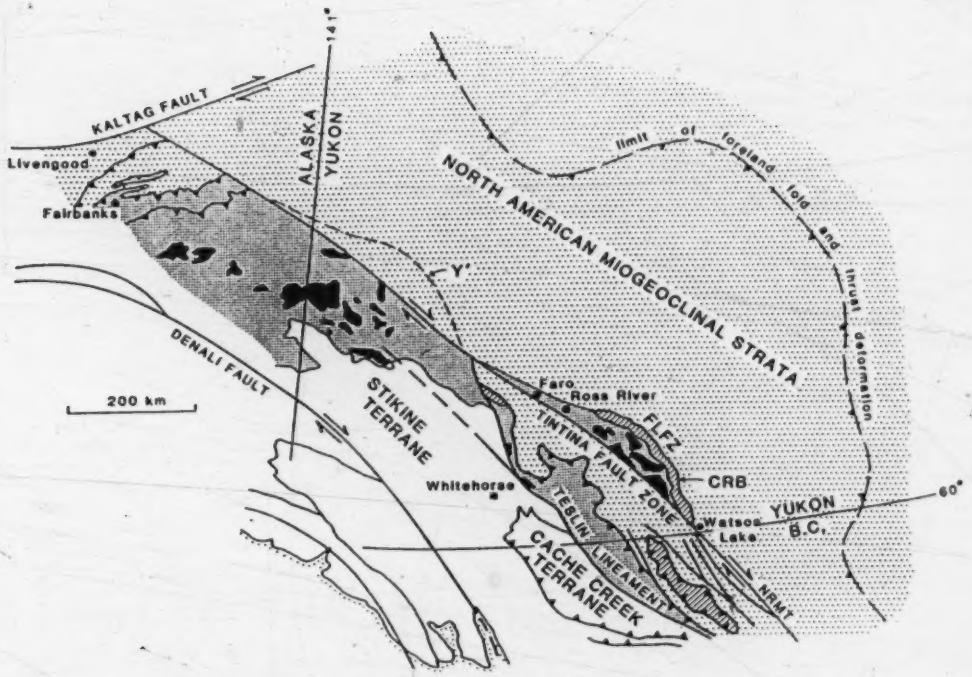

Figure 2.2. Map of the Yukon-Tanana terrane of the Yukon Territory and east-central Alaska and its bounding terranes. Yukon-Tanana terrane: dense stipple; North American miogeoclinal strata: open stipple; Slide Mountain terrane: ruled pattern; Mississippian orthogneisses: solid black; FLFZ = Finlayson Lake fault zone, NRMT = Northern Rocky Mountain Trench, CRB = Campbell Range belt. Dashed outline at Y' shows position of part of Yukon-Tanana terrane prior to being offset 450 km along the Tintina fault zone. (From Mortensen and Jilson, 1985.)

slices imbricated with the YTT (Mortensen, 1992). The Slide Mountain terrane forms a discontinuous belt that extends for nearly 4000 km along the length of the Cordillera (Roback et al., 1994). The Slide Mountain terrane is comprised of numerous individual allochthons, ranging from weakly metamorphosed to unmetamorphosed Mississippian to Permian basalt and a sedimentary sequence including chert, argillite, sandstone and conglomerate (Smith and Lambert, 1995). The Slide Mountain is generally considered to be the remnant of a marginal basin that separated the Quesnellia and Stikine island-arc terranes from North America (Tempelman-Kluit, 1979; Roback et al., 1994; Smith and Lambert, 1995).

The Cache Creek terrane has been divided into western, central and eastern belts, each of which constitutes a subterrane with slightly different lithology (Smith and Lambert, 1995). Basaltic rocks are found predominantly in the belt eastern (Bonaparte subterrane) in southern British Columbia. The central belt (Marble Range subterrane) is composed of Mid-Late Permian limestones and the western belt (Pavillion subterrane) contains mainly silicified argillite, siltstone, chert and minor limestones (Smith and Lambert, 1995). Unlike the Slide Mountain terrane, Tethyan faunas are found in the Cache Creek terrane and these indicate that parts of the terrane are far travelled relative to

North America (Mortensen, 1992; Smith and Lambert, 1995). The rocks of the Cache Creek terrane indicate an open-ocean environment and the terrane is probably the remains of a Paleo-Pacific ocean (Smith and Lambert, 1995). The Teslin fault separates the YTT from the Cache Creek terrane in the Yukon (Wheeler and McFeely, 1991).

2.3.2 Cassiar Terrane

The TTZ is juxtaposed against rocks of the pericratonic Cassiar terrane, which is a displaced portion of the Permo-Triassic margin of North American continental crust (Tempelman-Kluit, 1979; Hansen, 1989; Hansen, 1992b). Both the TTZ and Cassiar rocks are L-S tectonites (extemely sheared rocks displaying C and S fabrics in addition to lineations; Erdmer, 1985, Hansen, 1992b; Stevens and Erdmer, 1996). The Cassiar rocks range in metamorphic grade from unmetamorphosed to amphibolite facies (Hansen, 1992b) and little is known about its metamorphic evolution and its role in terrane accretion. Rocks of the Cassiar terrane range from Upper Proterozoic to Lower Cambrian clastic passive margin sediments, to Devonian to Mississippian continental shelf carbonates and shales and clastic sediments interfingered with volcanics, to Devonian to

Triassic diorite, and to Triassic to Jurassic shale, sandstone and carbonates (Wheeler and McFeely, 1991).

2.3.3 Quesnellia Terrane

Small slivers of the Quesnellia terrane are in fault contact with the Yukon-Tanana terrane along the Teslin fault (Erdmer et al., 1996). The Quesnellia terrane is one of the proposed island arc terranes of the Intermontane Belt and is composed of Late Devonian to Late Permian oceanic sedimentary rocks and Mid-Triassic to Early Jurassic volcanics.

2.3.4 North America

The YTT lies in thin structural sheets over the continental margin of North America. The presence of grey phyllite incorporated into slices of the terrane provides possible evidence of autochthonous rocks of the North American continental margin imbricated with the thrust sheets during terrane accretion (Erdmer, 1985; Hansen, 1989).

2.4 Local Geology

More than a dozen eclogite lenses are known in central Yukon within the YTT (Erdmer, 1987; refer to figure 1.1). Previous work by Erdmer and Helmstaedt (1983) and Erdmer (1987, 1988 and 1991) provides important information regarding local geology and petrography for the samples studied here and it is necessary for accurate interpretation of the geochemical results. This section provides a brief summary of the field relations from this previous work.

Approximately 10 km northwest of Faro, three lenses (I, II and III) of eclogite crop out (locality A in figure 1.1). The lenses are structurally interleaved with graphitic quartzite and siliceous blastomylonite of the Nisutlin Allochthon with contacts poorly exposed (Erdmer and Helmstaedt, 1983). Foliations within the eclogite and the host rock are parallel. Three samples representing each of the lenses were analyzed for major, trace and rare earth elements (PE-80-F1, PE-80-F2 and PE-80-F3). Pressure-temperature calculations for Faro eclogites suggest temperatures in the 400-500°C range with minimum pressure estimates at 11-13 kbars or possibly 15 kbars (Erdmer et al., in press). $^{40}Ar/^{39}Ar$ dating of white mica from a Faro eclogite (PE-80-F3) yielded dates of 256 ± 3

Ma and 261 ± 2 Ma (intergrated ages) and may have been overprinted in the Early Jurassic (Erdmer et al., in press).

An outcrop of eclogites, 20 km northwest of Ross River (locality B in figure 1.1), within a quartz-muscovite-glaucophane-garnet schist with well-developed blastomylonitic fabric and a chlorite-actinolite-plagioclase greenstone displaying schistose fabric, both of the Nisutlin Allochthon (Erdmer, 1987). Eclogite forms a number of lenses of varying sizes within the schist and contacts are sharp. Mylonitic fabric is present in the eclogite and the greenstone. Foliation in the eclogite and the schist is parallel. The samples evaluated for major, trace, and rare earth element in this thesis are PE-85-19 and PE-85-21. Pressure-temperature estimates for Ross River indicated that the eclogites equilibrated at a pressure of ~ 10 kbars at 470°C (Erdmer, 1987). New pressure-temperature calculations show that the eclogite (PE-85-21) reached 525°C and at least 13 kbars (Erdmer et al., in press). Erdmer et al. (in press) reported that intergrated $^{40}Ar/^{39}Ar$ mica dates for Ross River eclogite and blueschist samples of 274.2 ± 2.6 Ma and 272.3 ± 2.6 Ma, respectively. Subsequent dating of the same samples yielded intergrated $^{40}Ar/^{39}Ar$ mica dates of 267 ± 3 Ma and 273 ± 3 Ma, respectively.

Several small outcrops of eclogite occur 10 km west of Last Peak (Erdmer and Helmstaedt, 1983; locality C in figure 1.1). The eclogite is bounded by a lens of serpentinite of the Anvil Allochthon in the west and by hornblende-biotite schist of the Nisutlin Allochthon to the east. The contacts are not exposed but the authors believe the units to be structurally interleaved. As at Faro, foliation is parallel in the eclogite and the host rocks. Samples from Last Peak include PE-80-BSR and PE-80-BSRC. Calculation of pressure-temperature estimates for Faro and Last Peak eclogites gave variable results, but the pressures were interpreted to be at least 12 kbars at temperatures from 600-700°C during peak metamorphic conditions (Erdmer and Helmstaedt, 1983). However, later recalculation of the pressure by Erdmer (1987) gave pressures 2-3 kbars higherthan previous values, consistent with values from Ross River and Stewart Lake. Erdmer et al. (in press) reported a temperature of 605 ± 20°C and a minimum pressure of 14 kbars for an eclogite from Last Peak (PE-80-BSR). A date of 269 ± 2 Ma was obtained by U-Pb zircon dating of this sample (Creaser et al., 1997a).

Two clusters of eclogite outcrops are dispersed along several kilometres, centred 5 km south and 3 km northwest of Stewart Lake (locality E in figure 1.1). Additional eclogite outcrops occur along strike 10 km and 20 km to the south of Stewart Lake and 10

km to the northwest (Erdmer, 1987). The eclogite is hosted by a muscovite-quartz phyllite and varied metabasic rocks of the Anvil Allochthon. These rocks are part of a ductilely sheared klippe. Contacts are poorly exposed but are inferred by Erdmer (1987) to be tectonic in nature. Nine samples were collected from the Stewart Lake area (PE-85-10,PE-85-10B, PE-85-11-1, PE-85-11-2, PE-85-12, PE-85-16B, PE-85-17, PE-85-18, PE-85-18B). Pressure-temperature estimates for eclogites at Stewart Lake suggest that equilibration of the eclogites occurred at 12-15 kbars and 530-750°C (Erdmer, 1987). $^{40}Ar/^{39}Ar$ mica dating of eclogites, separated by 2 km, yielded two different dates. One is Early Carboniferous at 346 ± 3 Ma (PE-85-17) and the other is Triassic at 228 ± 1 Ma (PE-85-10) (Erdmer et al., in press).

The Simpson Range eclogite (CRE-95-205) is in a heavily retrogressed rock from an isolated exposure in the Simpson Range Mountains (Mortensen and Jilson, 1985). Several lenses of altered garnet metabasite and eclogite occur as resistant units within mylonitic metachert and minor greenstone (Erdmer et al., in press). These authors correlate the host rocks with Slide Mountain terrane. An date of 344 ± 1 Ma was obtained for this sample by $^{40}Ar/^{39}Ar$ mica dating (Erdmer et al., in press).

Chapter 3 Whole Rock Geochemistry

3.1 Introduction

In this chapter the geochemistry of the various eclogites is described, and the petrogenesis and tectonic setting of these rocks is interpreted. As eclogites, these rocks have undergone significant high-pressure and/or high-temperature metamorphism. Therefore interpretations relying on immobile trace and rare earth elements will be emphasized and those employing major elements will be used as a guide only.

Seventeen samples of eclogite from several different localities within the Yukon Tanana terrane were analyzed for major, trace and rare earth elements (Tables 2 and 3). The samples were chosen to provide reasonable coverage of the eclogite occurrences within the terrane. Twenty mineral separates (either garnet or pyroxene) were also analyzed for trace and rare earth elements (Table 4) primarily to determine REE contents for Sm-Nd geochemistry. The analyses were performed at Washington State University using x-ray fluorescence spectrometry (XRF) and inductively coupled plasma mass

Table 2

sample ID	PE-80-F1	PE-80-F2	PE-80-F3	PE-80-BSR	PE-80-BSRC	PE-85-10	PE-85-10B	PE-85-11-1	PE-85-11-2	PE-85-12	PE-85-16B	PE-85-17	PE-85-18	PE-85-18B	PE-85-19-4	PE-85-21-7	CRE-95-205	Avg. MORB
Unnormalized Results (Weight %):																		
SiO2	51.48	50.94	49.82	48.92	47.28	49.98	49.13	55.35	45.06	54.15	51.09	53.70	53.40	51.47	51.84	51.95	48.44	N/A
Al2O3	15.33	17.01	16.10	16.85	15.54	19.58	17.13	17.06	14.14	15.82	15.67	17.15	16.72	16.92	13.97	14.50	14.39	N/A
TiO2	1.430	0.844	1.753	2.040	2.396	0.350	0.288	0.621	0.449	0.556	1.245	0.555	0.607	0.636	1.646	1.955	1.154	N/A
FeO*	9.21	6.97	9.39	9.37	10.69	6.72	8.77	6.21	9.32	6.65	10.83	8.65	8.07	9.74	10.89	12.29	10.99	N/A
MnO	0.177	0.154	0.202	0.174	0.177	0.139	0.159	0.095	0.190	0.098	0.200	0.159	0.143	0.166	0.222	0.256	0.200	N/A
CaO	10.30	11.70	10.10	12.88	11.10	10.88	8.99	6.15	11.01	8.17	8.84	8.01	7.44	6.65	9.66	9.05	9.69	N/A
MgO	9.05	9.13	7.79	6.95	8.09	9.30	10.18	8.09	16.40	8.68	6.32	7.56	7.96	7.71	6.88	6.67	8.05	N/A
K2O	0.32	0.25	0.91	0.20	0.31	0.36	0.36	0.59	0.05	0.26	0.29	0.24	1.02	1.77	0.65	0.36	0.27	N/A
Na2O	2.99	2.71	3.85	2.37	2.99	3.46	3.44	5.48	0.94	5.09	3.25	5.27	4.13	3.73	2.85	3.42	2.92	N/A
P2O5	0.152	0.039	0.218	0.230	0.390	0.012	0.024	0.078	0.018	0.031	0.109	0.020	0.029	0.033	0.183	0.122	0.079	N/A
Total	100.44	99.75	100.13	99.98	98.87	100.78	98.47	99.72	97.58	99.51	97.84	101.31	99.52	98.82	98.79	100.57	96.18	N/A
Normalized Results (Weight %):																		
SiO_2	51.25	51.07	49.75	48.93	47.82	49.59	49.89	55.50	46.18	54.42	52.22	53.00	53.66	52.08	52.47	51.65	50.36	49.21
Al_2O_3	15.26	17.05	16.08	16.85	15.63	19.43	17.40	17.11	14.49	15.90	16.02	16.93	16.80	17.12	14.14	14.42	14.96	15.81
TiO_2	1.424	0.846	1.751	2.040	2.423	0.347	0.292	0.623	0.460	0.559	1.272	0.548	0.610	0.644	1.666	1.944	1.200	1.39
FeO*	9.17	6.99	9.38	9.37	10.81	6.67	8.91	6.23	9.55	6.68	11.07	8.54	8.11	9.85	11.02	12.22	11.42	7.19
MnO	0.176	0.154	0.202	0.174	0.179	0.138	0.161	0.095	0.195	0.098	0.204	0.157	0.144	0.168	0.225	0.25	0.208	0.16
CaO	10.25	11.73	10.09	12.88	11.23	10.80	9.13	6.17	11.28	8.21	9.03	7.91	7.48	6.73	9.78	9.00	10.07	11.14
MgO	9.01	9.15	7.78	6.95	8.18	9.23	10.34	8.11	16.81	8.72	6.46	7.46	8.00	7.80	6.96	6.63	8.37	8.53
K_2O	0.32	0.25	0.91	0.20	0.31	0.36	0.37	0.59	0.05	0.26	0.30	0.24	1.02	1.79	0.66	0.36	0.28	0.26
Na_2O	2.98	2.72	3.84	2.37	3.02	3.43	3.49	5.50	0.96	5.12	3.32	5.20	4.15	3.77	2.88	3.40	3.04	2.71
P_2O_5	0.151	0.039	0.218	0.230	0.394	0.012	0.024	0.078	0.018	0.031	0.111	0.020	0.029	0.033	0.185	0.121	0.082	0.15
Trace Elements in ppm:																		
Ni	145	139	78	285	152	72	103	84	323	81	25	113	57	44	39	35	72	100*
Cr	360	448	324	368	295	161	222	187	987	252	52	371	151	104	126	90	280	275*
Sc	39	33	40	30	36	46	36	28	44	25	35	43	30	34	37	47	39	40.6**
V	263	238	279	262	281	220	206	216	181	236	318	218	251	242	322	364	315	300*
Ba	347	158	1214	59	126	355	926	140	18	43	70	3	115	327	824	663	145	6.3*
Rb	7	9	21	3	4	8	6	6	0	2	3	4	16	32	12	9	7	0.56*
Sr	58	170	121	1015	221	193	346	106	45	96	56	52	63	70	131	187	221	90*
Zr	93	48	108	152	177	34	27	48	22	38	66	31	29	31	88	111	63	74*
Y	38	24	25	31	35	7	8	21	14	15	32	16	16	18	36	43	28	28*
Nb	4.1	3.1	8.7	9.1	21.3	1.9	1.2	3.3	2.6	3.2	0.9	1.6	1.4	0.0	4.3	4.4	2.5	2.33*
Ga	23	17	14	25	18	13	14	13	12	14	16	14	16	15	19	23	18	16*
Cu	55	64	0	67	53	3	29	9	154	10	92	50	86	75	48	60	54	87**
Zn	73	79	54	97	93	25	52	13	63	13	80	100	65	72	84	92	103	122**
Pb	0	0	2	3	2	54	7	0	0	0	0	0	0	0	0	3	0	0.3*
La	2	4	6	22	21	0	0	8	2	4	0	6	2	5	0	12	0	2.5*
Ce	4	4	0	27	41	2	0	15	20	0	16	6	22	0	7	10	7	7.5*
Th	2	1	2	0	1	0	0	1	0	1	3	1	1	1	0	1	3	0.12*
Group	FRS	FRS	BSR	BSR	BSR	SLC	SLC	SLC	cumulate	SLK	FRS	SLK	SLK	SLK	FRS	FRS	FRS	

Avg. MORB; **Pearce, 1982; * Pearce et al., 1995, remainder Melson and Thompson, 1971.

Table 3 **Whole Rock Samples**

	Trace and Rare Earth Elements in ppm:																							
Sample ID	**La**	**Ce**	**Pr**	**Nd**	**Sm**	**Eu**	**Gd**	**Tb**	**Dy**	**Ho**	**Er**	**Tm**	**Yb**	**Lu**	**Ba**	**Th**	**Nb**	**V**	**Hf**	**Ta**	**U**	**Pb**	**Rb**	**Cs**	**Sr**	**Sc**
PE-80-F1	3.92	10.86	1.81	9.70	3.78	1.39	5.28	1.05	7.00	1.49	4.44	0.61	3.72	0.57	367	0.24	3.04	39.96	2.55	0.18	0.08	0.68	7.96	0.28	62	39
PE-80-F2	1.60	4.36	0.83	4.63	2.04	0.86	3.01	0.63	4.14	0.92	2.70	0.37	2.32	0.36	163	0.10	0.93	24.33	1.15	0.06	0.08	2.55	8.83	0.53	181	33
PE-80-F3	3.35	6.86	1.01	4.59	1.37	0.58	2.23	0.56	4.31	0.99	2.94	0.41	2.55	0.42	1178	0.40	8.25	26.00	2.69	0.49	0.12	2.97	20.94	0.54	129	40
PE-80-BSR	13.21	29.71	4.06	19.53	7.20	3.91	8.51	1.35	7.10	1.30	3.44	0.47	2.79	0.41	71	0.56	9.96	33.00	3.14	0.61	0.87	3.98	2.47	0.05	1025	30
PE-BSRC	15.30	33.99	4.56	20.63	6.07	2.06	6.34	1.12	6.65	1.36	3.57	0.51	2.98	0.45	95	1.15	19.46	34.85	4.36	1.20	0.36	1.08	6.27	0.11	208	35
PE-85-10	2.55	4.93	0.69	3.14	1.24	0.51	1.45	0.23	1.39	0.29	0.85	0.12	0.82	0.14	359	0.26	0.71	7.00	0.66	0.04	0.05	51.89	7.93	0.45	208	46
PE-85-10B	1.21	2.29	0.41	1.86	0.88	0.47	1.27	0.25	1.36	0.29	0.82	0.13	0.79	0.12	871	0.16	0.36	7.67	0.33	0.02	0.08	6.49	7.00	0.25	314	50
PE-85-11-1	2.83	6.73	1.03	5.17	1.93	0.74	2.78	0.55	3.84	0.85	2.40	0.35	2.17	0.35	139	0.31	1.48	22.62	1.42	0.11	0.10	0.93	6.48	0.15	124	39
PE-85-11-2	3.96	7.46	0.99	4.04	1.26	0.47	1.77	0.36	2.43	0.55	1.61	0.23	1.45	0.24	12	0.70	0.78	14.12	0.58	0.05	0.12	1.02	0.93	0.05	51	51
PE-85-12	1.12	2.17	0.41	2.09	1.02	0.48	1.85	0.40	2.70	0.59	1.66	0.24	1.54	0.24	38	0.09	0.90	15.47	0.99	0.06	0.04	0.53	2.38	0.13	108	34
PE-87-16B	2.69	7.32	1.27	7.16	2.83	1.04	4.04	0.79	5.38	1.18	3.35	0.51	3.25	0.49	59	0.23	1.11	32.60	1.67	0.08	0.14	1.59	5.10	0.13	81	43
PE-85-17	0.78	1.84	0.33	1.66	0.82	0.40	1.65	0.41	2.80	0.61	1.89	0.27	1.71	0.27	25	0.07	0.39	16.65	0.74	0.03	0.04	0.48	3.28	0.10	59	43
PE-85-18	0.82	1.85	0.38	2.03	1.05	0.46	1.86	0.43	3.08	0.68	1.94	0.28	1.78	0.28	112	0.08	0.30	17.92	0.87	0.03	0.03	0.84	16.39	0.34	71	42
PE-85-18B	0.80	2.03	0.41	2.51	1.29	0.52	2.07	0.42	3.10	0.70	2.08	0.31	1.97	0.31	60	0.20	1.08	32.71	1.81	0.07	0.13	0.81	4.70	0.13	139	43
PE-85-19-4	3.47	9.24	1.53	8.17	3.30	1.34	5.07	0.99	6.66	1.43	3.94	0.56	3.51	0.55	726	0.17	2.56	37.13	2.33	0.18	0.11	2.15	13.32	0.46	146	47
PE-85-21-7	5.27	14.4	2.29	12.18	4.32	1.58	5.96	1.16	7.57	1.60	4.78	0.67	4.19	0.64	646	0.24	3.25	45.32	2.81	0.21	0.13	3.76	9.21	0.76	200	47
CRE-95-205	2.34	5.73	1.02	5.65	2.32	0.92	3.33	0.69	5.11	1.12	3.17	0.46	2.87	0.45	133	0.11	1.65	28.46	1.68	0.11	0.09	1.64	8.30	0.25	223	53.2
Avg. MORB	2.5	7.5	1.32	7.3	2.63	1.02	3.68	0.67	4.55	1.01	2.97	0.456	3.05	0.455	6.3	0.12	2.33	28	2.05	0.13	0.047	0.3	0.56	0.007	90	40

Table 4 **Mineral Separates**

Trace and Rare Earth Elements in ppm:

Sample ID	La	Ce	Pr	Nd	Sm	Eu	Gd	Tb	Dy	Ho	Er	Tm	Yb	Lu	Ba	Th	Nb	Y	Hf	Ta	U	Pb	Rb	Cs	Sr	Sc
PE-80-F1-px	2.08	4.57	0.92	4.42	1.82	0.70	2.93	0.56	3.82	0.81	2.14	0.27	1.50	0.24	115	0.11	1.98	23.71	0.42	0.12	0.05	1.88	3.5	0.21	82	49.02
PE-80-F1-gl	0.68	1.58	0.30	1.50	1.40	1.08	6.21	1.79	14.83	3.57	11.48	1.83	12.56	1.98	31	0.04	1.29	96.15	0.58	0.09	0.04	1.72	1.0	0.03	20	113.17
PE-80-F2-px	1.66	3.29	0.73	3.52	1.48	0.63	2.26	0.42	3.00	0.67	1.90	0.27	1.67	0.27	125	0.09	0.73	18.92	0.25	0.05	0.07	1.12	7.2	0.40	133	47.65
PE-80-F2-gl	0.57	1.22	0.25	1.18	0.95	0.65	4.09	1.19	9.66	2.29	7.11	1.18	8.13	1.24	29	0.04	0.61	60.51	0.39	0.05	0.03	0.57	1.9	0.11	36	84.20
PE-80-F3-pl	3.08	5.41	0.94	3.90	1.19	0.40	1.28	0.15	0.79	0.13	0.31	0.04	0.30	0.05	277	0.23	4.19	3.51	0.77	0.25	0.11	1.23	3.2	0.21	62	30.95
PE-80-F3-gl	0.69	1.21	0.21	0.88	0.82	0.82	5.82	1.97	17.74	4.15	12.20	1.84	12.12	1.87	62	0.05	4.55	110.50	0.73	0.29	0.06	0.44	1.4	0.08	18	110.77
PE-80-F3-p2	37.24	80.38	11.61	56.01	16.55	5.01	14.68	1.43	4.50	0.44	0.65	0.07	0.44	0.06	58	3.53	8.18	10.75	0.97	0.49	1.34	6.72	1.0	0.10	251	30.32
PE-85-17-px	0.69	1.00	0.29	1.42	0.75	0.22	0.66	0.09	0.54	0.10	0.25	0.03	0.23	0.03	16	0.03	0.29	2.94	0.21	0.02	0.03	0.16	2.3	0.08	56	24.89
PE-85-17-gl	1.17	3.29	0.56	2.94	1.61	0.95	4.61	1.10	8.62	2.03	6.21	0.96	6.41	1.03	14	0.13	0.34	54.03	0.21	0.03	0.09	0.14	2.3	0.09	21	100.56
PE-80-BSR-gl	7.27	14.97	1.87	8.48	3.40	1.69	6.60	1.65	13.71	3.16	9.05	1.27	7.95	1.20	37	0.47	22.48	80.53	0.94	1.40	0.24	0.34	3.7	0.16	31	45.56
PE-80-BSR-g2	7.55	15.56	1.93	8.93	3.37	1.66	6.37	1.60	13.64	3.15	8.81	1.27	7.86	1.17	47	0.49	20.52	81.68	0.71	1.34	0.25	0.20	4.3	0.18	38	46.09
PE-80-BSR-px	14.41	31.97	4.35	21.09	6.38	2.44	7.69	1.27	7.81	1.48	3.69	0.49	2.96	0.44	70	0.85	11.87	37.54	0.95	0.77	0.26	1.45	6.7	0.20	306	38.77
KF-95-10-p1	30.58	61.64	7.51	31.93	7.29	2.10	4.41	0.41	1.61	0.23	0.46	0.05	0.32	0.04	74	2.46	23.77	5.54	0.85	1.50	0.63	2.04	5.6	0.83	338	25.95
KF-95-10-p2	29.59	59.60	7.34	31.52	6.83	1.96	4.16	0.38	1.44	0.19	0.37	0.05	0.27	0.03	61	2.29	21.73	4.98	0.86	1.29	0.60	1.98	4.9	0.78	315	26.19
KF-95-10-gl	26.61	55.71	6.43	27.25	7.07	2.85	11.48	2.54	16.45	3.02	7.00	0.85	4.78	0.64	63	1.99	35.18	69.48	2.27	2.18	0.59	0.71	6.1	0.99	126	26.80
KF-95-10-g2	22.78	47.62	5.64	24.44	6.49	2.82	11.78	2.59	16.58	2.96	6.90	0.85	4.95	0.67	63	1.89	82.51	69.55	2.28	4.90	0.61	0.76	6.3	1.04	110	26.17
PE-85-21-p1	2.72	6.47	1.12	5.66	1.98	0.53	1.60	0.16	0.82	0.15	0.39	0.06	0.40	0.06	478	0.11	2.39	4.18	0.52	0.16	0.09	2.61	7.2	0.42	140	33.92
PE-85-21-p2	2.24	5.38	0.95	4.96	1.73	0.52	1.42	0.14	0.76	0.14	0.37	0.05	0.36	0.05	435	1.10	1.76	4.17	0.32	0.10	0.08	2.73	7.4	0.37	156	35.09
PE-85-21-g1	0.29	0.66	0.13	0.77	2.18	2.08	11.81	2.91	20.31	4.43	12.71	1.88	11.56	1.67	71	0.03	1.31	113.96	0.55	0.09	0.05	0.34	2.7	0.07	14	98.64
PE-85-21-g2	0.32	0.68	0.14	0.79	2.18	2.10	12.33	2.96	20.00	4.40	12.87	1.85	11.19	1.62	70	0.02	1.28	116.26	0.50	0.09	0.04	0.44	3.5	0.07	14	92.39

spectrometry (ICP-MS) (Hooper et al., 1993). Major elements are reported as oxides in weight percent and trace and rare earth elements in parts per million (ppm).

3.2 Major Element Variations

The average silica value for the eclogites is 50.97%. The lowest silica value is 45.06% and the highest value is 55.35%, both of these are Stewart Lake samples.

The grouping of the eclogites seen in the TiO_2 and P_2O_5 diagrams corresponds to groups FRS, SLC/K and BSR. Faro, Ross River and Simpson Range eclogites form group FRS, Stewart Lake eclogites groups SLC and SLK and Last Peak eclogites and PE-80-F3 (Faro) group BSR. These groups were determined on the basis of trace and rare earth element data given below.

On a TiO_2 versus SiO_2 diagram (figure 3.1A), the samples form two groupings. Eclogites from Last Peak and Faro (group BSR) plot in a line with negative slope. Faro, Ross River and Simpson Range (group FRS) form a cluster with slight positive correlation. Samples from Stewart Lake (groups SLC and SLK) show no correlation with silica and are significantly lower in TiO_2.

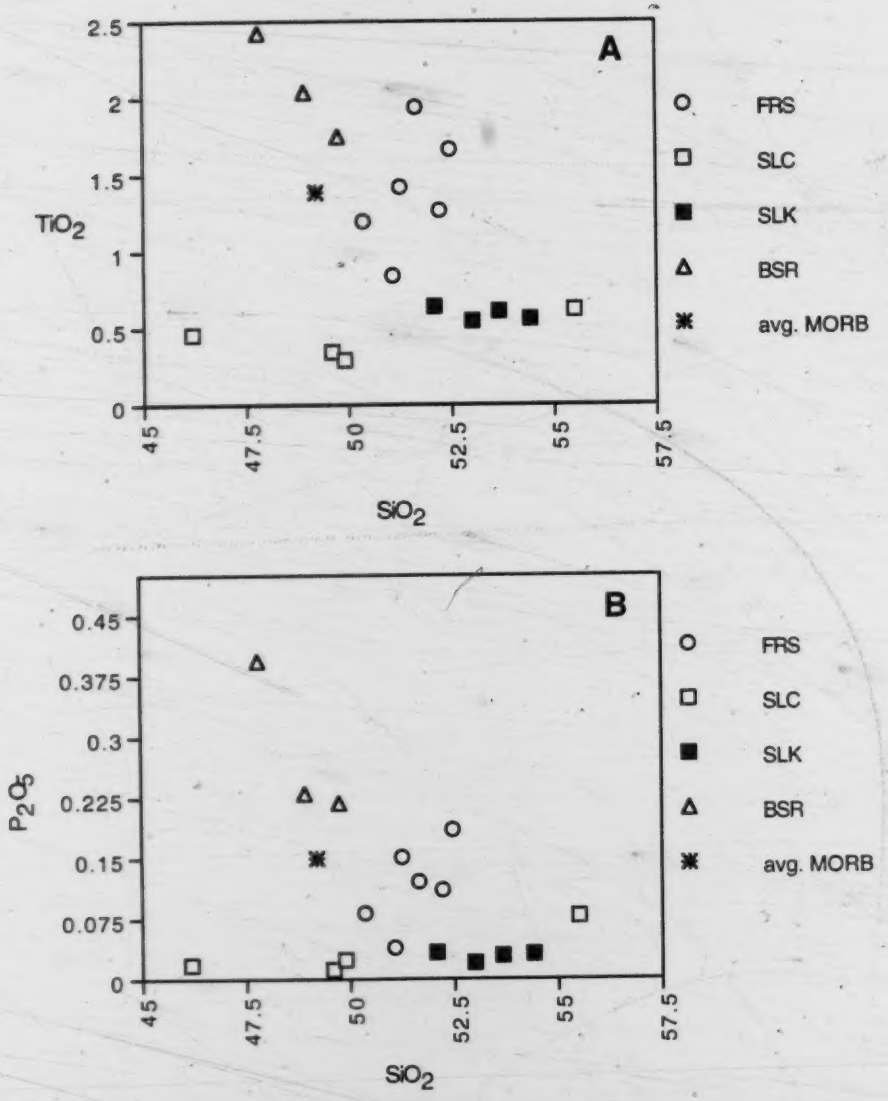

Figure 3.1. Harker variation diagrams for Yukon-Tanana eclogites. A = TiO_2 versus silica. B = P_2O_5 versus silica. (modified from Harker, 1904.)

Three distinct groupings are formed on a P_2O_5 versus SiO_2 plot (figure 3.1B). Eclogites from group BSR display negative correlation with silica. Group FRS forms a cluster with positive correlation with SiO_2. Stewart Lake eclogites (groups SLC and SLK) are significantly lower in P_2O_5 and show no correlation with SiO_2. Apatite is present as an accessory mineral in some of the samples.

On the FeO* (total iron calculated as FeO; figure 3.2A) versus SiO_2 plot the Stewart Lake samples can be separated into two distinct groups (SLC and SLK) each showing a negative correlation with silica. Eclogites from group BSR also display a negative correlation. Group FRS is more scattered with exhibit slight positive correlation with SiO_2.

The Stewart Lake eclogites are also divisible into two groups (SLC and SLK) on a MgO versus SiO_2 plot (figure 3.2B). Half of the Stewart Lake samples show positive correlation with SiO_2 (SLK) and a negative correlation with silica is displayed by the remaining samples (SLC). Negative correlation with SiO_2 is also displayed by group FRS. Group BSR shows no variation with silica.

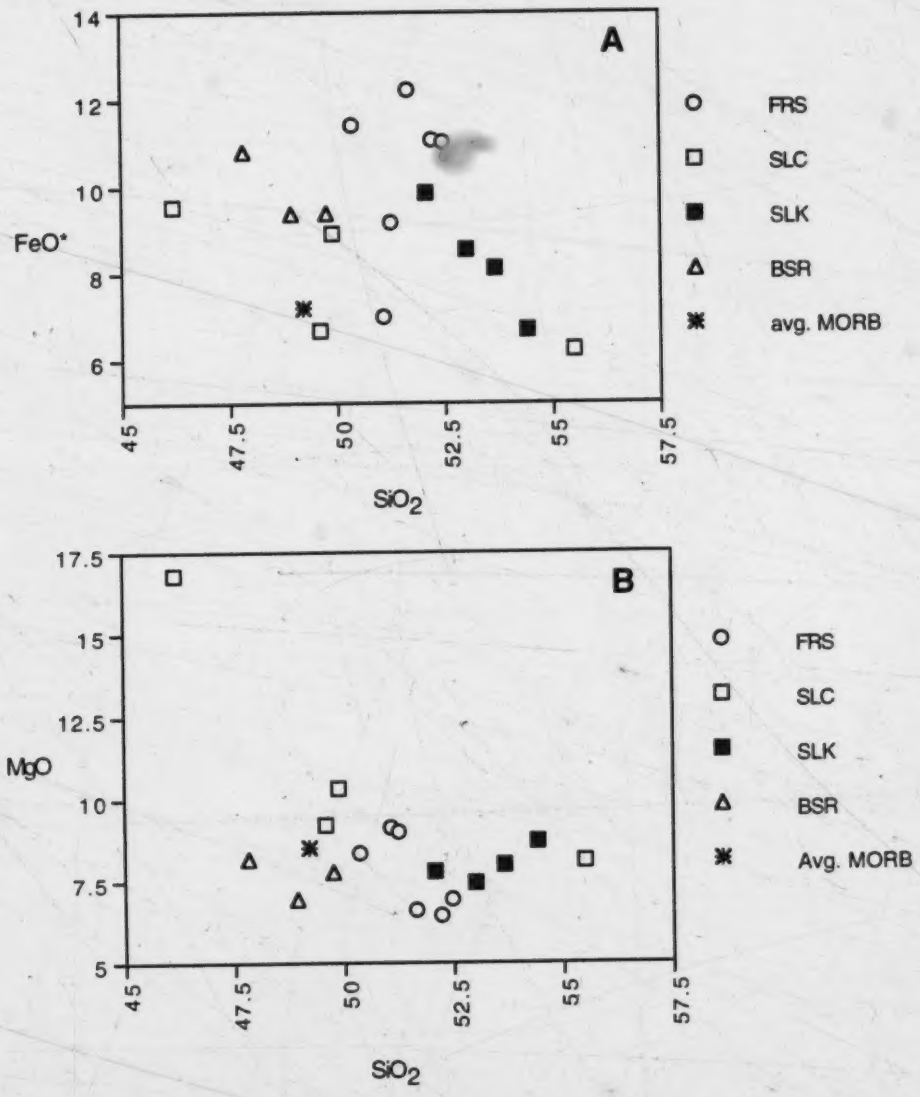

Figure 3.2. Harker variation diagrams for Yukon-Tanana eclogites. A= FeO* versus silica. B = MgO versus silica. (modified from Harker, 1904.)

MnO (figure 3.3A) versus SiO_2 plots Stewart Lake eclogites also separate into two groups each exhibiting negative correlation with silica. The remaining samples from groups BSR and FRS show slight positive correlation with SiO_2. Groups BSR, FRS, and SLC display negative correlation with silica on a CaO versus SiO_2 plot (figure 3.3B). Positive correlation with SiO_2 is exhibited by group SLK for CaO

No correlation with SiO_2 is displayed by eclogites from groups BSR, FRS, SLC and SLK on a K_2O versus silica diagram (figure 3.4A). Less scatter is displayed by the various samples on a Na_2O versus SiO_2 diagram (figure 3.4B) and each group exhibits positive correlation with silica.

Two trends are displayed on a plot of Al_2O_3 versus silica (figure 3.5). Eclogites from groups BSR and SLC show positive correlation with SiO_2 and a negative correlation is displayed by the remainder of the samples from groups FRS and SLK. The Harker variations diagrams for the eclogites support the division of the samples into four distinct groups.

On the AFM diagram (figure 3.6) after Irvine and Baragar (1971) the eclogites from Faro with one exception (PE-80-F3), Last Peak, Ross River and Simpson Range plot

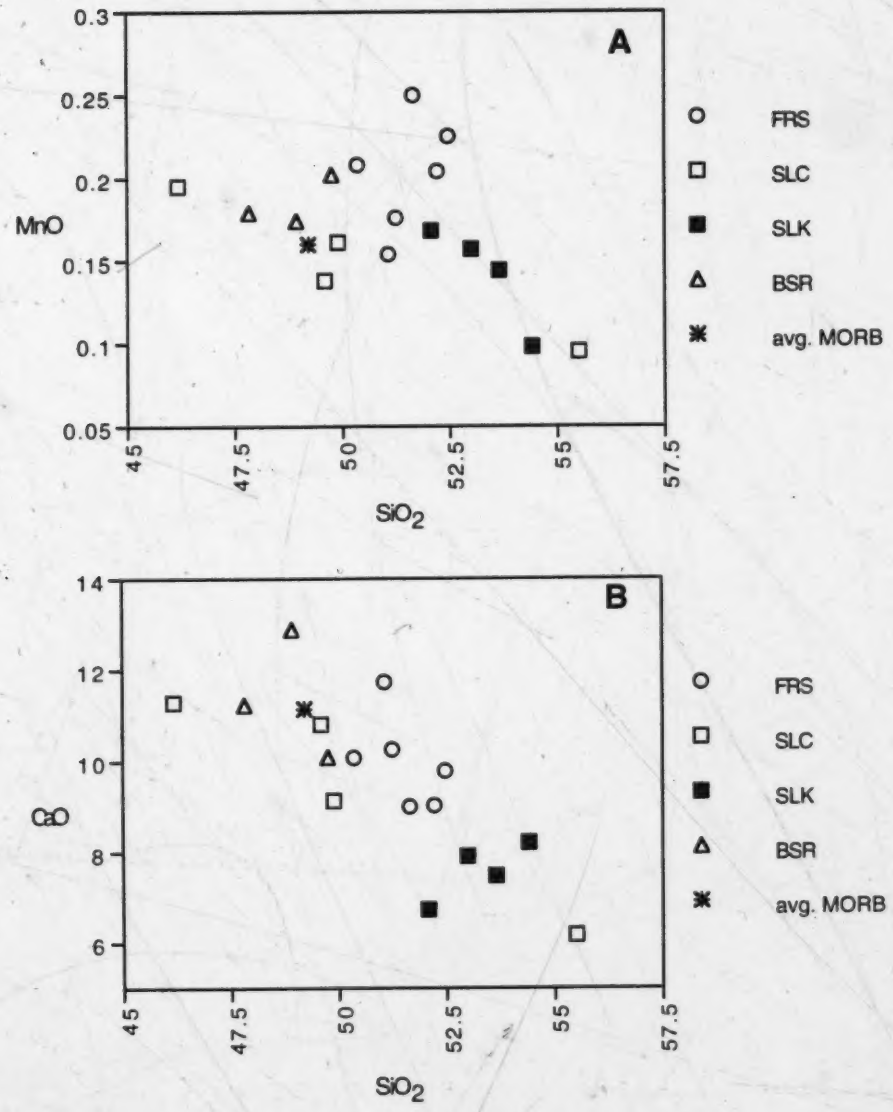

Figure 3.3. Harker variation diagrams for Yukon-Tanana eclogites. A = MnO versus silica. B = CaO versus silica. (modified from Harker, 1904.)

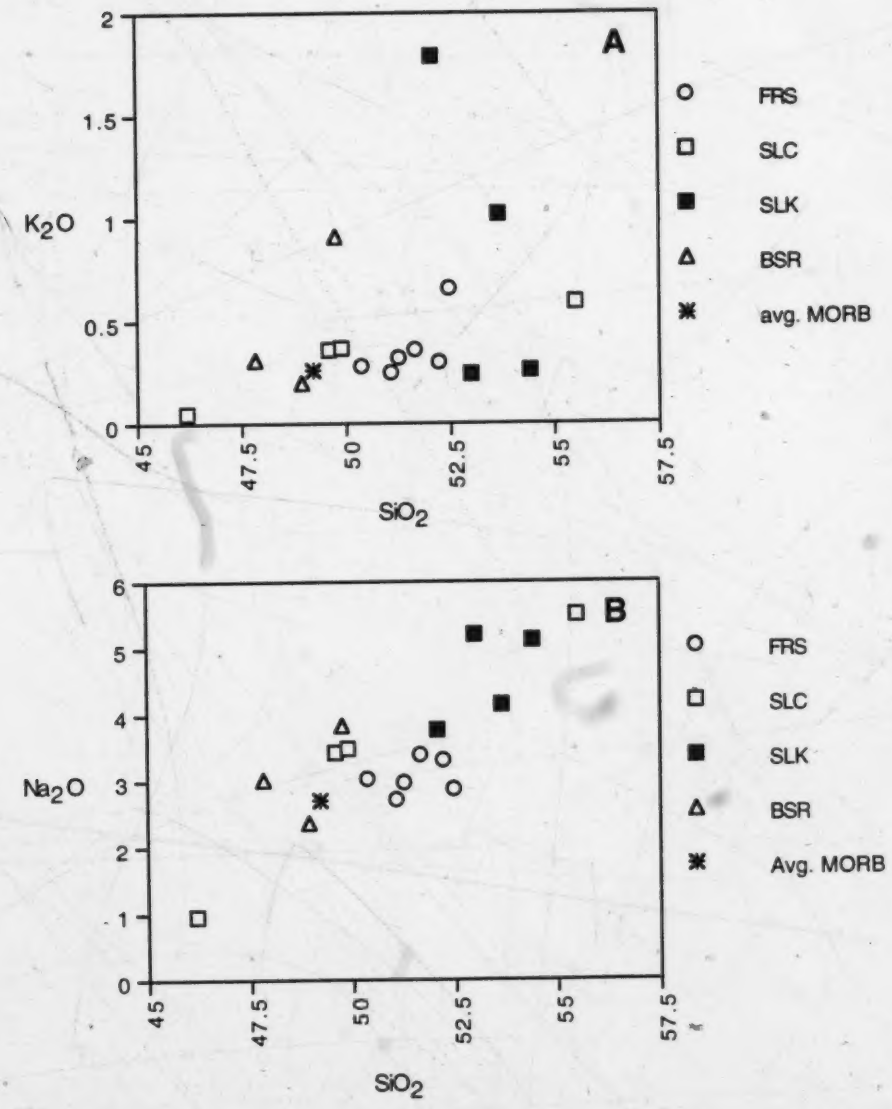

Figure 3.4. Harker variation diagrams for Yukon-Tanana eclogites. A = K_2O versus silica. B = Na_2O versus silica. (modified from Harker, 1904.)

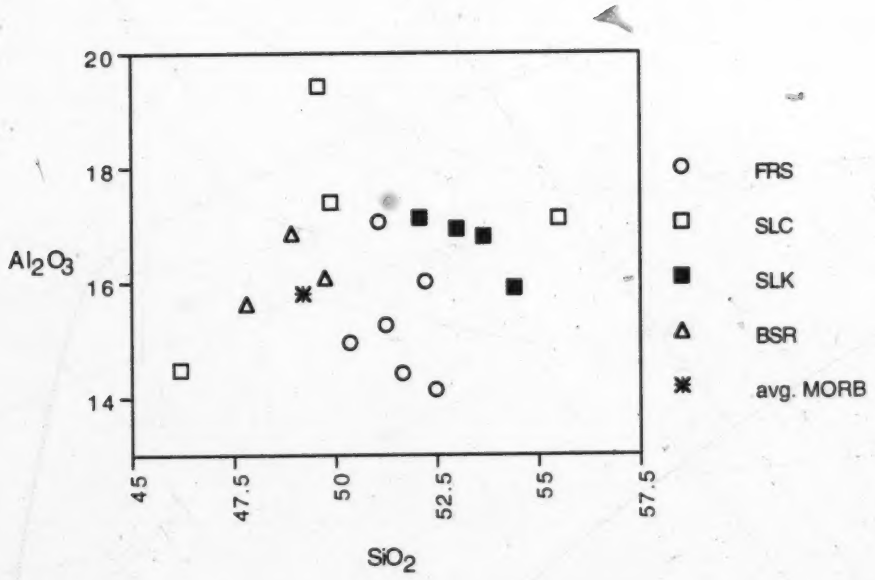

Figure 3.5. Harker variation diagram for Yukon-Tanana eclogites. Al_2O_5 versus silica. (modified from Harker, 1904.)

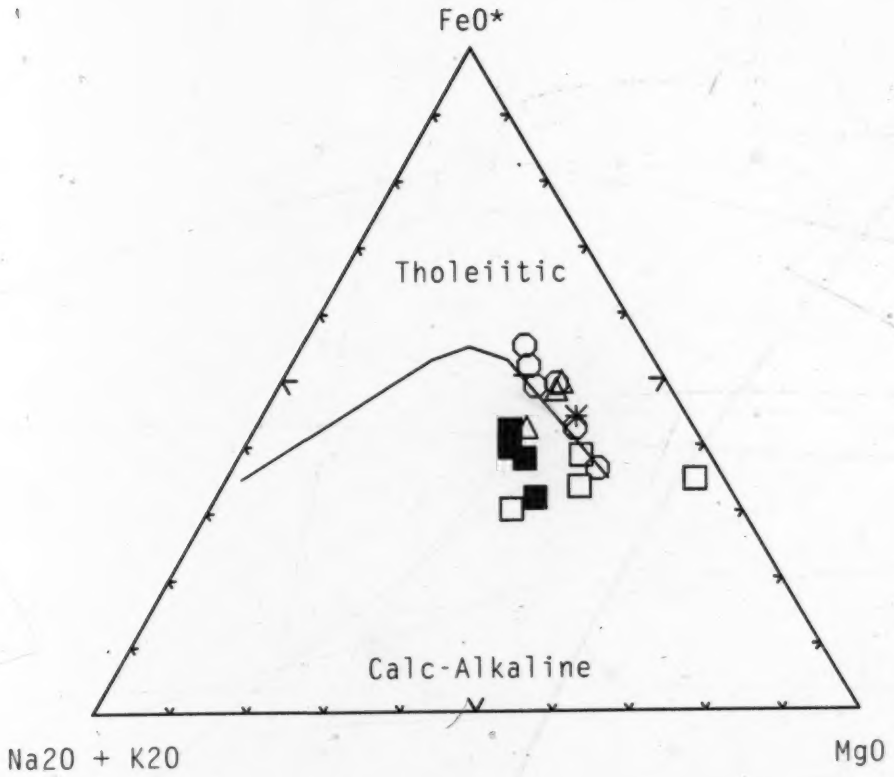

Figure 3.6. AFM diagram for Yukon-Tanana terrane eclogites. Distinguishes tholeiitic and calc-alkaline basalts. Group FRS = open circles; group SLC = open squares; group SLK = filled squares; group BSR = open triangles; avg. MORB = star. Group FRS = samples PE-80-F1, PE-80-F2, PE-85-16B, PE-85-19-4, PE-85-21-7, and CRE-95-205; group SLC = samples PE=85-10, PE-85-10B, PE-85-11-1, and PE-85-11-2; group SLK = samples PE-85-12, PE-85-17, PE-85-18, and PE-85-18B; group BSR = samples PE-80-F3, PE-80-BSR, and PE-80-BSRC. Fields defined by Irvine and Baragar, 1971.

in or on the line of the tholeiitic field. Samples from Stewart Lake plot within the calc-alkaline field with one exception, PE-85-11-2 which is likely a cumulate.

3.3 Chemical Affinity and Tectonic Setting

The tectonic settings of the andesitic/basaltic protoliths of the eclogites were determined using trace element abundances and ratios (e.g., Pearce and Cann, 1973; Pearce and Norry, 1979; Pearce, 1983; Shervais, 1982). Multielement and rare earth element spider diagrams normalized to n-MORB (Pearce, 1983) were also utilized. The results from these techniques indicate that the samples can be divided into four distinct groups, with eclogites from Stewart Lake forming groups SLC and SLK, Faro, Ross River and Simpson Range eclogites group FRS and Last Peak (Big Salmon River) group BSR.

Comparison of immobile trace element concentrations in older rocks with concentrations in present day volcanic rocks of known tectonic setting has been useful in identifying the tectonic setting (Pearce and Cann, 1973). Ti, Zr, Nb and Y contents of basalts vary systematically with tectonic setting (Pearce and Norry, 1979).

The degree of differentiation and magma series can be characterized for altered or metamorphosed rocks using immobile elements such as Ti, Zr, Y, Nb (Winchester and Floyd, 1977). On a plot of Zr/TiO_2 versus Nb/Y, the Nb/Y ratio and the Zr/TiO_2 ratio are indices of alkalinity but only Zr/TiO_2 represents a differentiation index. Samples from Faro, Ross River and Stewart Lake plot within the andesite/basalt field of the subalkaline series on the Zr/TiO_2 versus Nb/Y diagram (figure 3.7). Eclogites from Last Peak and sample PE-80-F3 plot just below the line as subalkaline basalts, trending toward alkaline basalts.

The Ti/100-Zr-Y*3 diagram (figure 3.8) from Pearce and Cann (1973) discriminates between "within-plate" basalts (continental and oceanic) and other basalt types for altered and metamorphosed samples. Groups SLC, SLK, and FRS do not plot as "within-plate" basalts. Eclogites from group BSR and PE-80-F3 (Faro) plot in the "within-plate" field.

The Ti-Zr diagram (figure 3.9; Pearce and Cann, 1973) further distinguishes basalt types that are not within-plate basalts. Ocean-floor basalts (MORB) plot in fields B and D, low-potassium tholeiites in fields A and B and calc-alkaline basalts in fields A and C. Groups SLC and SLK plots in field A. Group FRS plot within fields B and D. The very

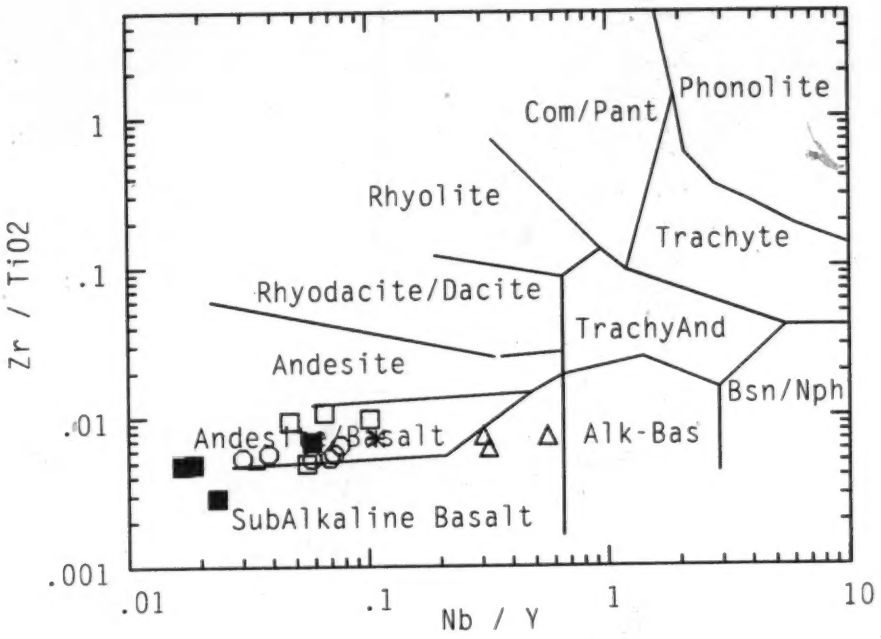

Figure 3.7. Zr/TiO_2 versus Nb/Y diagram for Yukon-Tanana terrane eclogites. Distinguishes degree of differentiation and magma series for metamorphosed rocks. Group FRS = open circles; group SLC = open squares; group SLK = filled squares; group BSR = open triangles; avg. MORB = star. Samples in each group as listed in caption of figure 3.6 Fields defined by Winchester and Floyd (1977.).

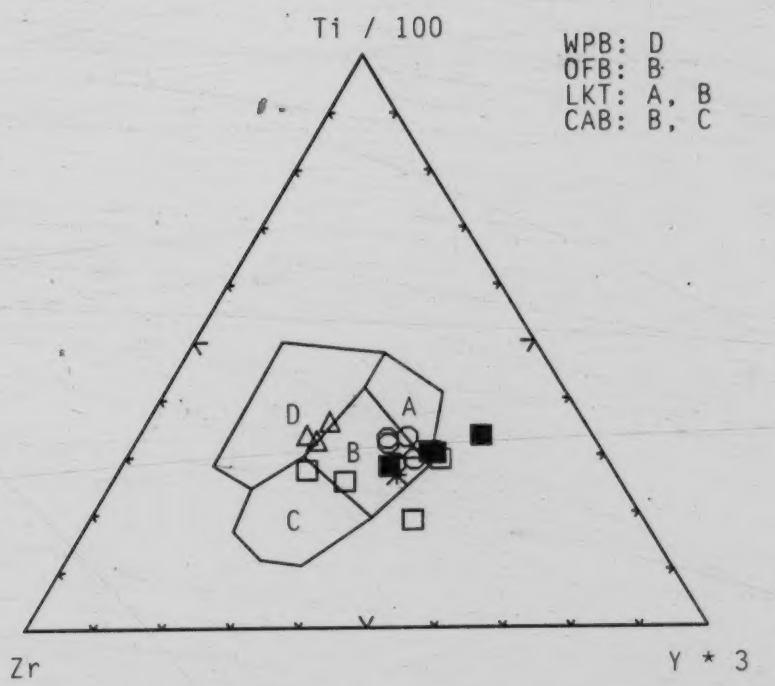

Figure 3.8. Ti-Zr-Y diagram for Yukon-Tanana terrane eclogites. Discriminates between "within-plate" basalts (continental and oceanic) and other basalt types for altered or metamorphosed rocks. WPB = within-plate basalt; OFB = ocean floor basalt (equivalent to MORB); LKT = low-K tholeiite; CAB = calc-alkaline basalt. Group FRS = open circles; group SLC = open squares; group SLK = filled squares; group BSR = open triangles; avg. MORB = star. Samples in each group as listed in caption of figure 3.6. Fields defined by Pearce and Cann (1973)..

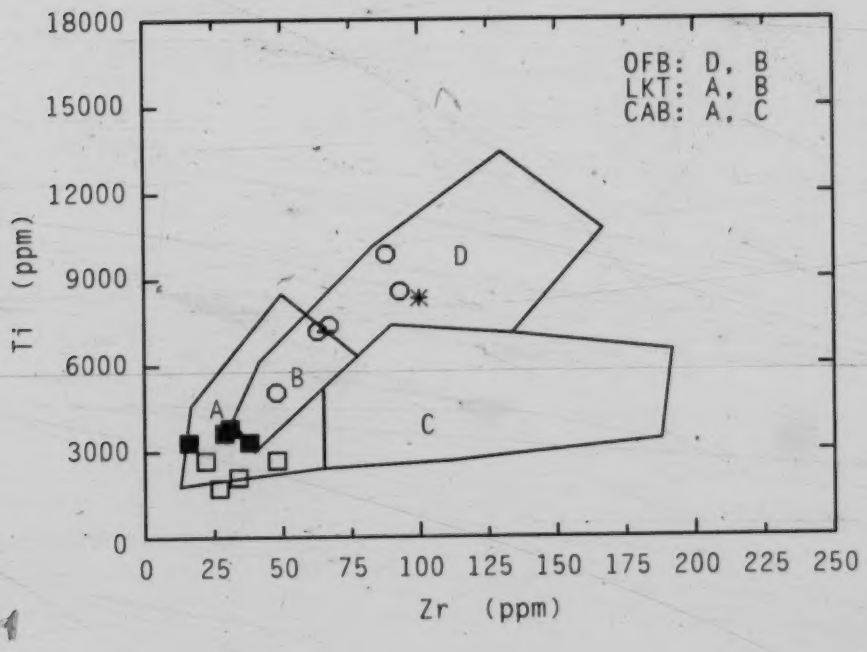

Figure 3.9. Plot of Ti versus Zr for Yukon-Tanana terrane eclogites further distinguishes basalt type. OFB = ocean floor basalt (equivalent to MORB); LKT = low-K tholeiite; CAB = calc-alkaline basalt. Group FRS = open circles; group SLC = open squares; group SLK = filled squares; group BSR = open triangles; avg. MORB = star. Samples in each group as listed in caption of figure 3.6. Fields defined by Pearce and Cann, 1973.

low values of Ti and Zr for the Stewart Lake eclogites are consistent with an island-arc setting (Pearce and Norry,1979), and the FRS eclogites with a n-MORB setting.

The Ti/V ratio can also be used for tectonic discrimination in altered or metamorphosed samples because Ti and V show coherent behaviour during alteration so that the Ti/V ratio remains approximately the same in the altered rock as in the fresh rock (Shervais, 1982). The ratio varies from 10-20 for arc related magmas, between 20 and 50 for n-MORB regardless of whether they are "normal" or "enriched" in LREE and LIL, and greater than 50 for within plate basalts. Ti/V ratios for groups SLC and SLK range from 8-16 indicating clear arc affinity (figure 3.10). Group FRS plots in the n-MORB range with values of 21-33. Group BSR and PE-80-F3 have the highest Ti/V ratios of the YTT eclogites and plot close to or within the within-plate basalt range.

The ratios Th/Yb and Ta/Yb (Pearce, 1983) and Zr/Y (Pearce and Norry, 1979) are also useful tectonic indicators. The Th/Yb ratios for calc-alkaline arc basalts are between 0.4 and 4 (table 1), whereas tholeiitic arc basalts have Th/Yb ratios less than 0.4. All arc basalts have Th/Yb ratios < 0.1. Ratios for groups SLC and SLK eclogites range from 0.04-0.48 which is consistent with their island-arc character. As shown by the major element diagrams, Stewart Lake eclogites form two groups on a Th/Yb-Ta/Yb plot

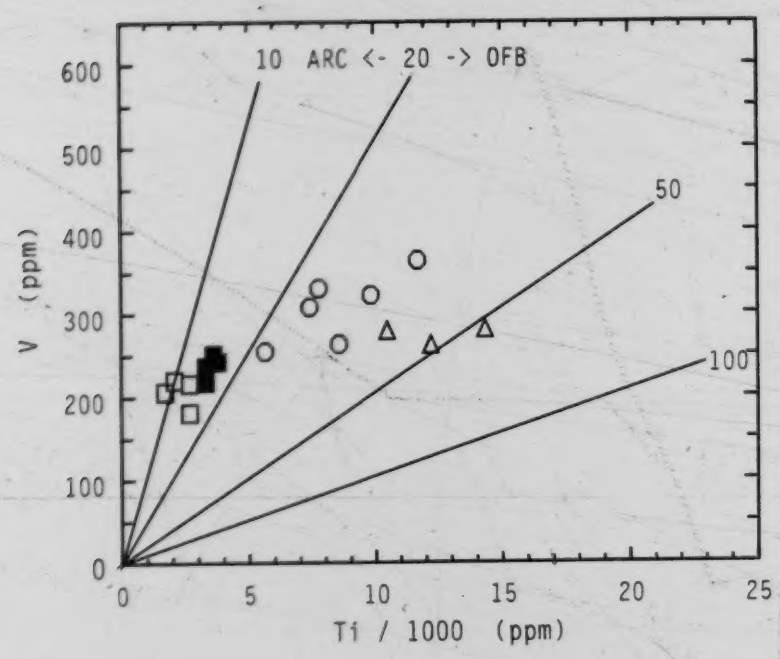

Figure 3.10. Plot of Ti versus V for Yukon-Tanana terrane eclogites. The Ti/V ratio is used for tectonic discrimination. It varies from 10-20 for arc related magmas to ~30 for n-MORB and to >50 for within-plate basalts. OFB = ocean-floor basalt (equivalent to MORB). Group FRS = open circles; group SLC = open squares; group SLK = filled squares; group BSR = open triangles; avg. MORB = star. Samples in each group as listed in caption of figure 3.6. Fields defined by Shervais, 1982.

(figure 3.11). Half of the samples have low Th/Yb and the remainder, with one exception, have higher Th/Yb and follow the subduction zone enrichment trend. One Stewart Lake sample (PE-85-16B) plots as MORB, which is consistent with all other geochemical indicators. Sample PE-85-16B also falls within the n-MORB fields on figures 3.9 and 3.12. The Th/Yb range for group FRS is 0.04-0.06 and the samples fall in the tholeiitic, n-MORB field. Sample PE-80-F3 and group BSR ratios follow the within-plate enrichment trend. Group BSR eclogites have high Ta/Yb ratios and are therefore within-plate basalts.

Pearce and Norry (1979) found island arc basalts have slightly lower Zr/Y ratios and lower mean Zr contents than mid-ocean ridge basalts. On the Zr/Y versus Zr diagram (figure 3.12) group SL plots in mainly the island-arc field with little overlap, and group FRS falls in the mid-ocean ridge basalt field. Within-plate characteristics are displayed by group BSR and PE-80-F3.

On the basis of immobile trace element ratios and contents a very consistent pattern emerges (table 5: summary of tectonic discrimination results; table 6); groups SLC and SLK are clearly of oceanic island-arc affinity, normal mid-ocean ridge basalt

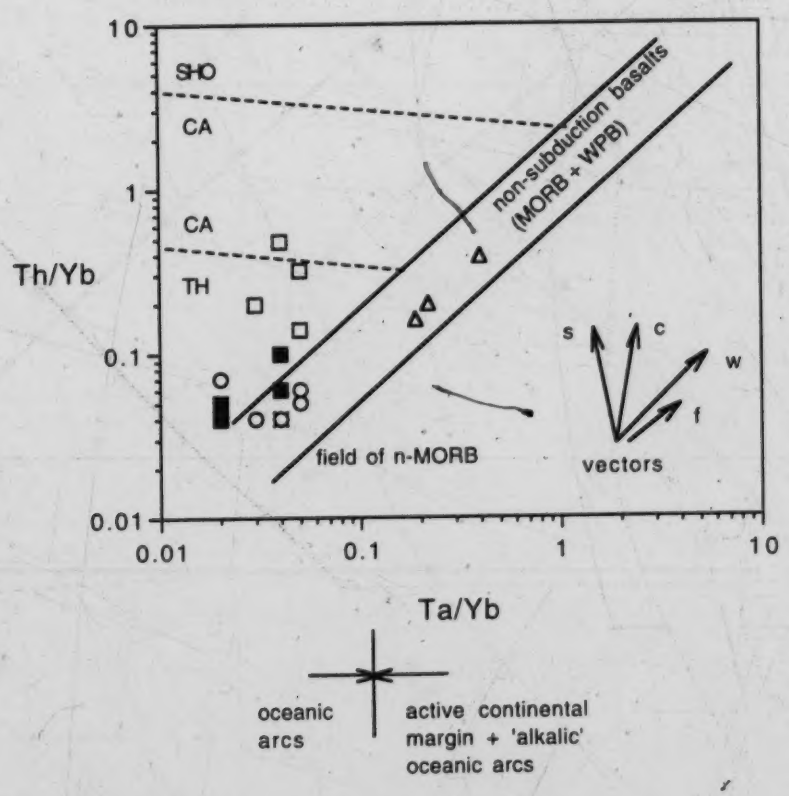

Figure 3.11. Th/Yb - Ta/Yb diagram for Yukon-Tanana eclogites distinguishing n-MORB, within-plate basalts and arc basalts. Vectors: s = subduction zone enrichment, c = crustal contamination, w = within-plate enrichment, f = fractional crystallization (for F = 0.5). Tholeiitic (TH), calc-alkaline (CA) and shoshonitic (SHO) boundaries for arc basalts taken from Pearce (1982) remaining fields and vectors defined by Pearce (1983). Group FRS = open circles; group SLC = open squares; group SLK = filled squares; group BSR = open triangles; avg. MORB = star. Samples in each group as defined in caption of figure 3.6.

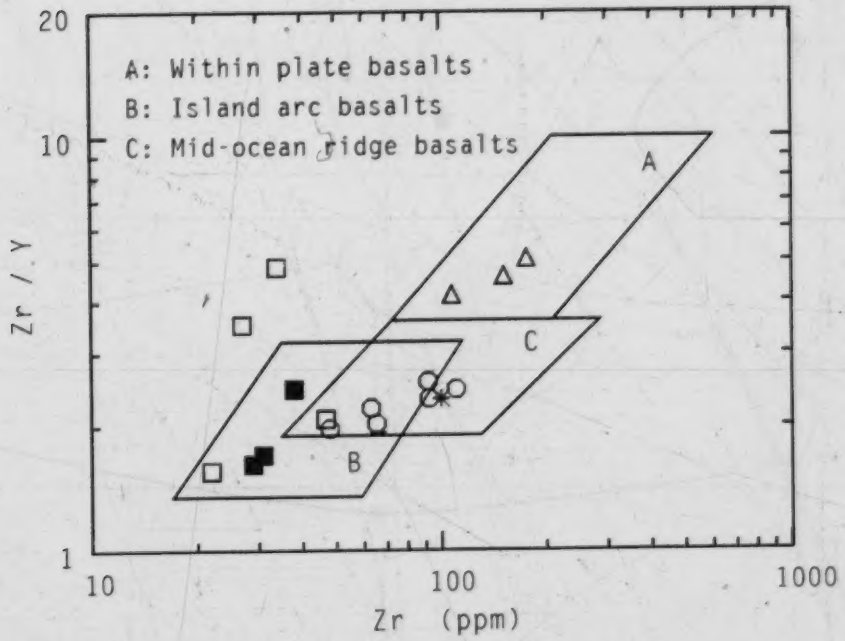

Figure 3.12. Zr/Y-Zr diagram for Yukon-Tanana terrane eclogites. Zr/Y ratio used for tectonic discrimination to further distinguish basalt type. Group FRS = open circles; group SLC = open squares; group SLK = filled squares; group BSR = open triangles; avg. MORB = star. Samples in each group as listed in caption of figure 3.6. Fields defined by Pearce and Norry (1979).

Table 5

Summary of tectonic discrimination diagram results

group	figure 3.6	figure 3.8	figure 3.9	figure 3.10	figure 3.11	figure 3.12
FRS	tholeiitic	MORB	MORB	MORB	MORB	MORB
SLC	calc-alkaline	CAB & OFB	CAB or LKT	Arc	CAB-Th Arc	Arc
SLK	calc-alkaline	LKT & OFB	CAB or LKT	Arc	Th Arc	Arc
BRS	tholeiitic	WPB	N/A	WPB	WPB	WPB

*Th = tholeiitic

Table 6

sample ID	protolith	Ti	Zr	V	Th	Ta	Yb	Y	Nb	Ti/Zr	Ti/V	Th/Yb	Ta/Yb	Zr/Y	Nb/Y
PE-80-F1	n-MORB	8573	93	263	0.24	0.18	3.72	39.96	3.04	92.2	32.6	0.06	0.05	2.33	0.08
PE-80-F2	n-MORB	5060	48	238	0.10	0.06	2.32	24.33	0.93	105.4	21.3	0.04	0.03	1.97	0.04
PE-80-F3	within-plate	10509	108	279	0.40	0.49	2.55	26.00	8.25	97.3	37.7	0.16	0.19	4.15	0.32
PE-80-BSR	within-plate	12230	152	262	0.56	0.61	2.79	33.00	9.96	80.5	46.7	0.20	0.22	4.61	0.30
PE-80-BSRC	within-plate	14364	177	281	1.15	1.20	2.98	34.85	19.46	81.2	51.1	0.39	0.40	5.08	0.56
PE-85-10	calc-alkaline	2098	34	220	0.26	0.04	0.82	7.00	0.71	61.7	9.5	0.32	0.05	4.86	0.10
PE-85-10B	calc-alkaline	1727	27	206	0.16	0.02	0.79	7.67	0.36	64.0	8.4	0.20	0.03	3.52	0.05
PE-85-11-1	calc-alkaline	2692	48	216	0.31	0.11	2.17	22.62	1.48	56.1	12.5	0.14	0.05	2.12	0.07
PE-85-11-2	calc-alkaline	2692	22	181	0.70	0.05	1.45	14.12	0.78	122.4	14.9	0.48	0.04	1.56	0.06
PE-85-12	low-K tholeiite	3333	38	236	0.09	0.06	1.54	15.47	0.90	87.7	14.1	0.06	0.04	2.46	0.06
PE-85-16B	n-MORB	7464	66	318	0.23	0.08	3.25	32.60	1.11	113.1	23.5	0.07	0.02	2.02	0.03
PE-85-17	low-K tholeiite	3327	16	218	0.07	0.03	1.71	16.65	0.39	207.9	15.3	0.04	0.02	0.96	0.02
PE-85-18	low-K tholeiite	3639	29	251	0.08	0.03	1.78	17.92	0.30	125.5	14.5	0.05	0.02	1.62	0.02
PE-85-18B	low-K tholeiite	3813	31	242	0.20	0.07	1.97	32.71	1.08	123.0	15.8	0.10	0.04	0.95	0.03
PE-85-19-4	n-MORB	9868	88	322	0.17	0.18	3.51	37.13	2.56	112.1	30.6	0.05	0.05	2.37	0.07
PE-85-21-7	n-MORB	11720	111	364	0.24	0.21	4.19	45.32	3.25	105.6	32.2	0.06	0.05	2.45	0.07
CRE-95-205	n-MORB	7194	63	315	0.11	0.11	2.87	28	1.60	114.2	22.8	0.04	0.04	2.25	0.06
SSM 1-3	low-K tholeiite		16.9	279	0.14	0.02	1.01	10.1	0.21			0.14	0.02	1.67	0.02
SST 5-1	calc-alkaline		85.7	277	1.34	0.16	3.42	32.7	2.09			0.39	0.05	2.62	0.06

characteristics are displayed by group FRS, and group BSR (including PE-80-F3) shows strong within-plate characteristics

3.4 Rare Earth Elements

Chondrite-normalized rare earth element diagrams are an important tool in determining the tectonic affinity of basaltic rocks because rocks of similar origins display consistent patterns on REE diagrams. REE diagrams for the eclogites (figure 3.13) clearly separate the samples into four distinct groups and further support the evidence from the tectonic discrimination diagrams described above. Stewart Lake eclogites are divided into group SLC with calc-alkaline island-arc character and group SLK with low potassium tholeiitic island-arc affinity; this grouping mimics that seen in the Th/Yb-Ta/Yb diagram (figure 3.11). Group FRS includes normal MORBs and eclogites from group BSR display within-plate character.

The SLC eclogites (figure 3.13A) are enriched in the LREEs (light rare earth elements) and are flat to slightly depleted in HREEs (heavy rare earth elements) with values ranging from 8-15 times that of chondrite, similar to an example of a modern

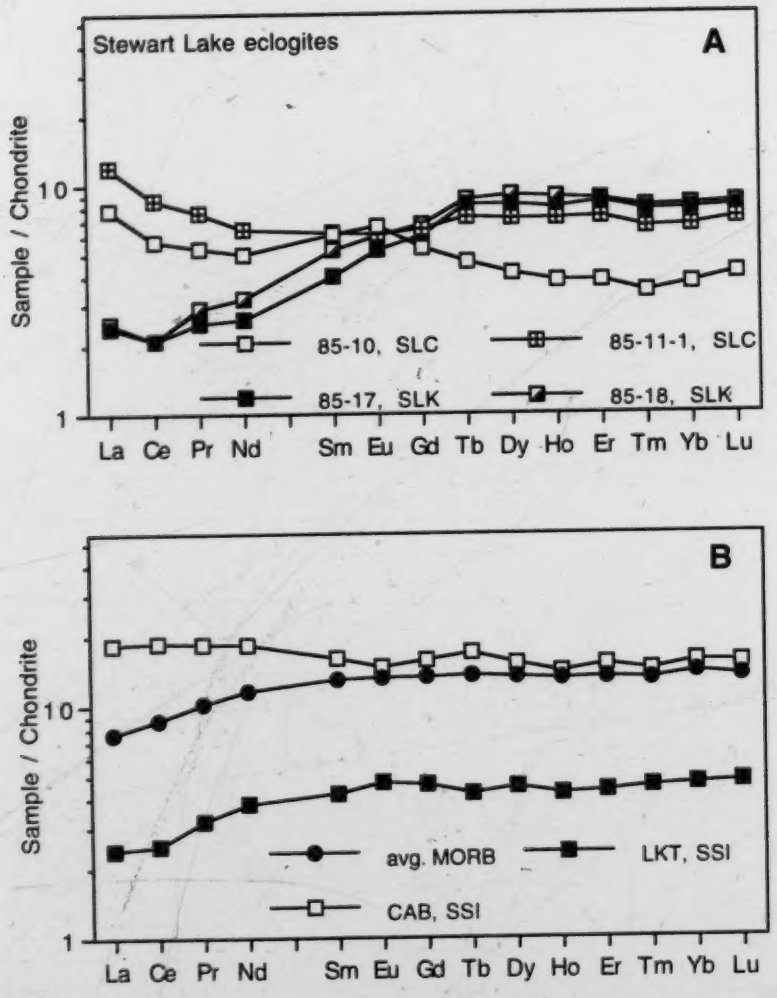

Figure 3.13. REE diagrams for groups SLC and SLK = A and average MORB (Pearce and Parkinson, 1993) and low-K tholeiite (LKT) and calc-alkaline basaltic andesite (CAB) from the South Sandwich Islands (Pearce et al., 1995) = B. Chondrite values from Newpet (1994). (La; 0.3290, Ce; 0.8650, Pr; 0.1300, Nd; 0.6300, Sm; 0.2030, Eu; 0.0770, Gd; 0.2760, Tb; 0.0498, Dy; 0.3430, Ho; 0.0770, Er; 0.2250, Tm; 0.0352, Yb; 0.2200, Lu; 0.0339).

calc-alkaline island-arc andesitic basalt from the South Sandwich Islands (figure 3.13B; Pearce et al., 1995). Group SLK (figure 3.13A) of low-potassium tholeiitic island-arc affinity are very depleted in the LREEs and enriched to flat in the HREEs. Values range from 2-10 times chondrite and the samples display the same pattern as an example from the South Sandwich Islands (figure 3.13B; Pearce et al., 1995).

Comparison of group FRS REE patterns (figure 3.14 a) with one of a normal MORB (figure 3.14 b; Pearce, 1983) shows identical patterns for each with a primarily flat pattern and slight LREE depletion and values at approximately 10 times that of chondrite.

Group BSR does not resemble the patterns for the previous groups. Comparison of the REE pattern for PE-80-BSR (figure 3.15B) with MORB shows strong enrichment in LREEs and a positive Eu anomaly. PE-80-F3 displays less enrichment in LREEs and no Eu anomaly. This sample may be more transitional than the rest of group BSR. Values range from 10-50 times chondrite for LREEs to 10-20 times chondrite for HREEs. The higher Th, Ta and Nb values are consistent with within-plate affinity (Pearce, 1983).

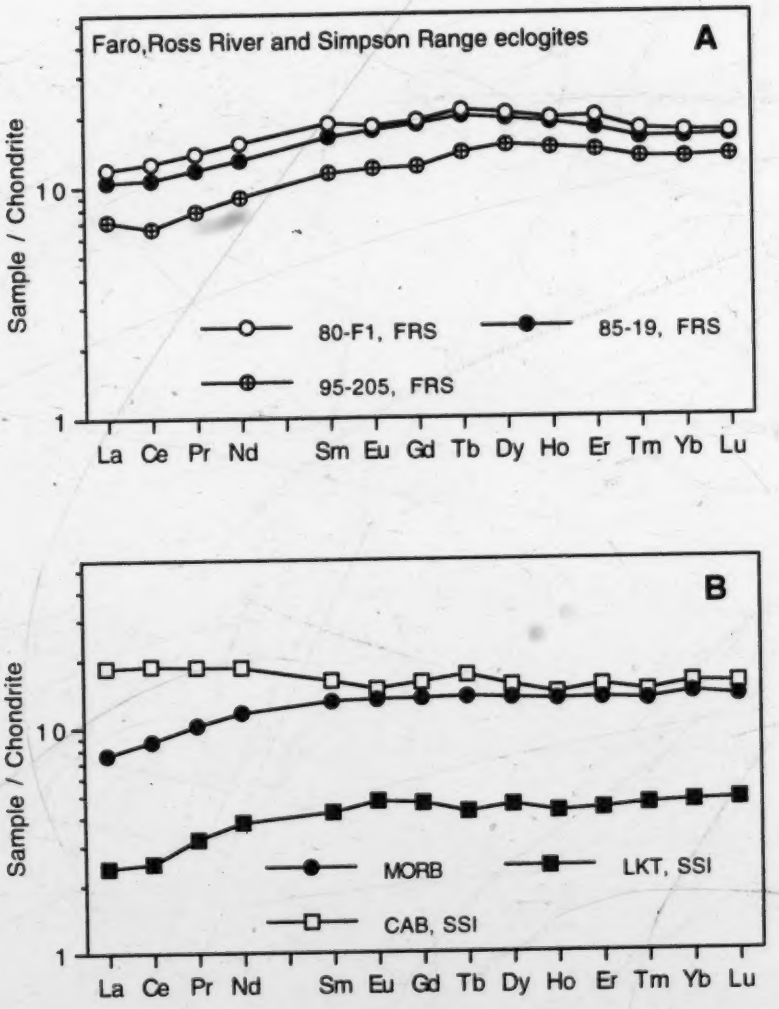

Figure 3.14. REE diagrams for group FRS = A and average MORB (Pearce and Parkinson, 1993) and low-K tholeiite (LKT) and calc-alkaline basaltic andesite (CAB) from the South Sandwich Islands (Pearce et al., 1995) = B. Chondrite values from Newpet (1994). (La; 0.3290, Ce; 0.8650, Pr; 0.1300, Nd; 0.6300, Sm; 0.2030, Eu; 0.0770, Gd; 0.2760, Tb; 0.0498, Dy; 0.3430, Ho; 0.0770, Er; 0.2250, Tm; 0.0352, Yb; 0.2200, Lu; 0.0339).

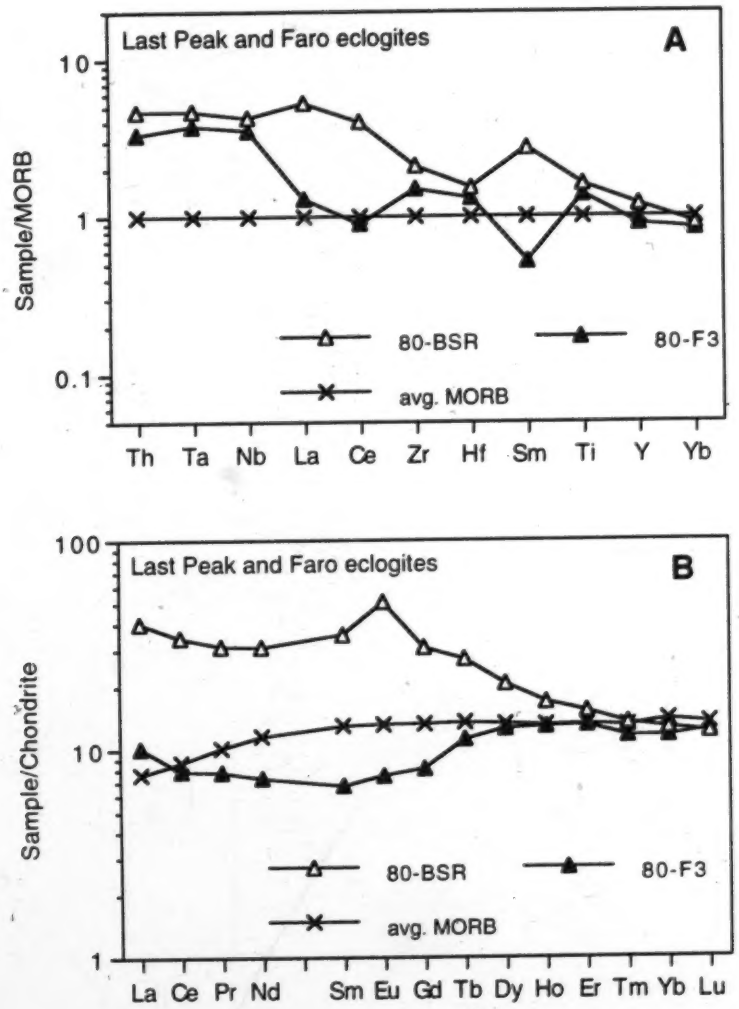

Figure 3.15. MORB-normalized incompatible element diagram and REE diagram for group BSR eclogites. A = Incompatible element diagram for group BSR and average MORB. Average MORB and normalizing values from Pearce and Parkinson (1993). B = REE diagram for group BSR and average MORB. Chondrite values from Newpet (1994). (La; 0.3290, Ce; 0.8650, Pr; 0.1300, Nd; 0.6300, Sm; 0.2030, Eu; 0.0770, Gd; 0.2760, Tb; 0.0498, Dy; 0.3430, Ho; 0.0770, Er; 0.2250, Tm; 0.0352, Yb; 0.2200, Lu; 0.0339).

3.5 Incompatible Elements

Basalts from various tectonic settings have well-defined patterns on MORB-normalized multielement diagrams (Pearce, 1983; Pearce and Parkinson, 1993; and Pearce et al., 1995). Comparison of incompatible element diagrams for the various samples with modern examples from the South Sandwich Islands (Pearce et al., 1995) strongly supports their subdivision into four groups of differing tectonic affinity.

Samples from Stewart Lake display patterns similar to oceanic island-arcs but can also be divided into low-potassium tholeiites and calc-alkaline basalts. PE-85-10, PE-85-10B, PE-85-11-1 and PE-85-11-2 (cumulate) (group SLC) clearly resemble calc-alkaline basalts with enrichment in Th, La and Ce and strong depletion in Ta and Nb (figures 3.16A). The remaining elements display a relatively flat pattern and values range from 0.5-8. They also have slightly higher silica values than other Stewart Lake eclogites and are therefore more andesitic than basaltic. These patterns are consistent with modern examples of calc-alkaline oceanic island-arc basaltic andesite from the South Sandwich Islands (figure 3.16B). PE-85-12, PE-85-17, PE-85-18 and PE-85-18B, (group SLK; figure 3.16A), however, display patterns typical of low-potassium tholeiites from the

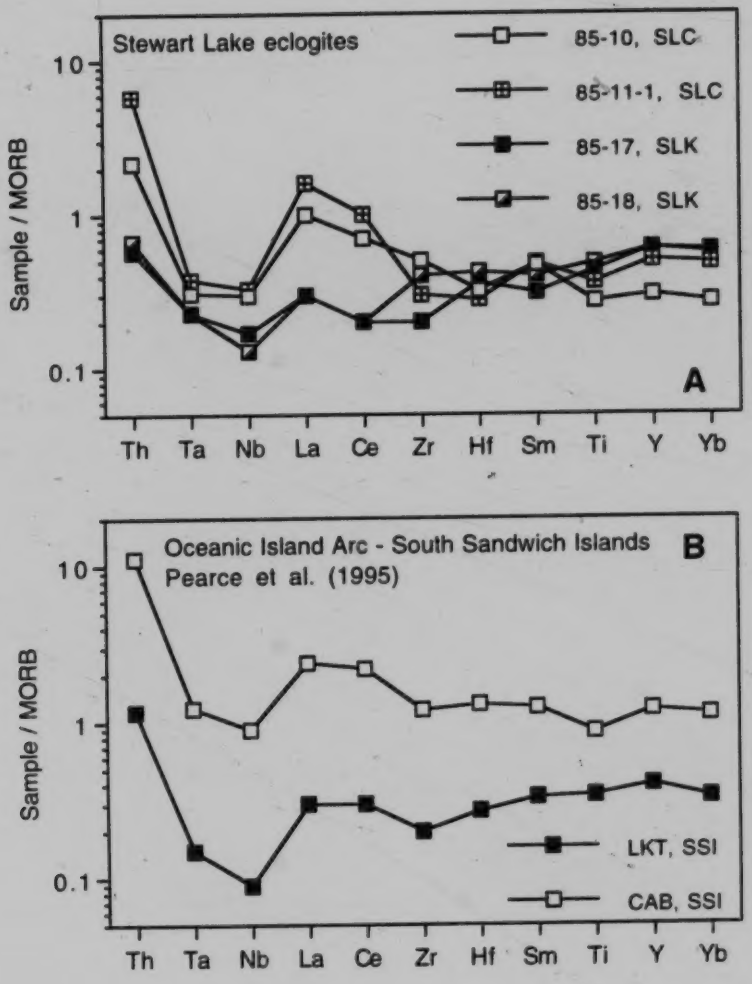

Figure 3.16. A = MORB normalized incompatible element diagram for Stewart Lake eclogites (groups SLC and SLK). Normalizing values from Pearce and Parkinson (1993). B = Incompatible element diagram for low-K tholeiite (LKT) and calc-alkaline basaltic andesite (CAB) from an oceanic arc setting (Pearce et al., 1995).

South Sandwich Islands (figure 3.16B). These samples are enriched in Th and La, strongly depleted in Ta and Nb and the remaining elements are flat and values range from 0.1-1.

Comparison of eclogites from group FRS (figure 3.17A) to the examples from the South Sandwich Islands(figure 3.17B) reveals totally different patterns on the incompatible element diagram to those of groups SLC or SLK. These samples have the very flat patterns typical of average mid-ocean ridge basalts. Values for the various elements are approximately 1 and are thus identical to MORB.

On an incompatible element diagram (figure 3.15A), group BSR eclogites display enrichment in Th, Ta and Nb and increasing depletion in the remaining elements, unlike the island-arc examples. This is consistent with their classification as within-plate basalts. PE-80-F3 shows greater depletion in La and Ce and Sm and may reflect a more transitional character.

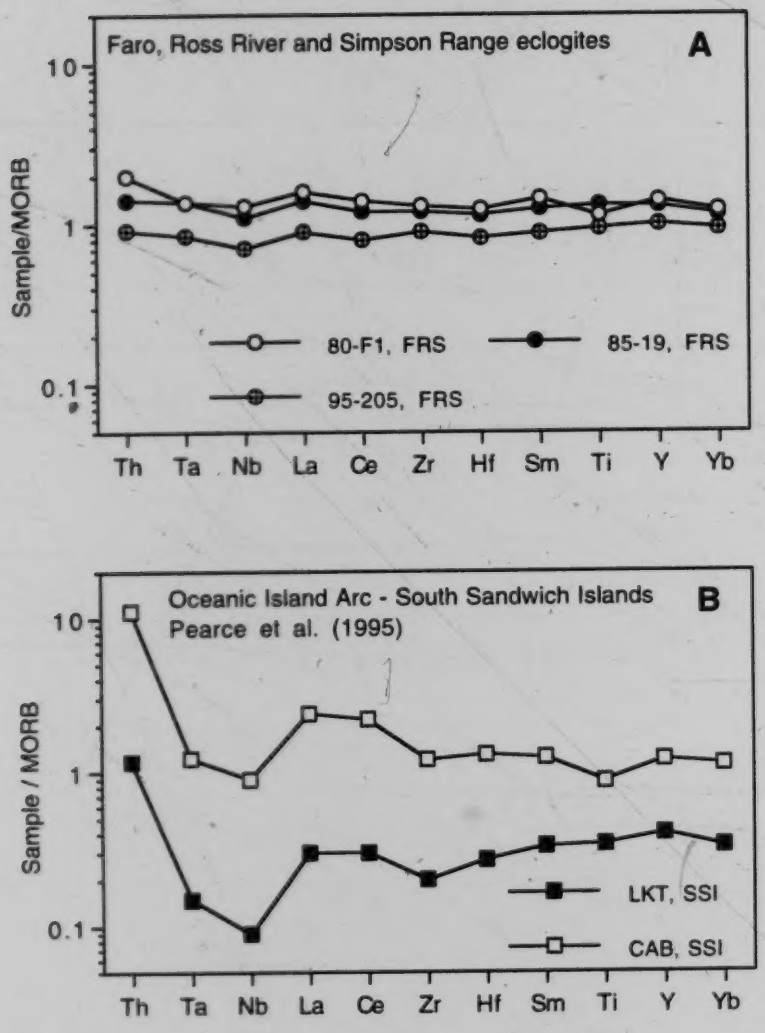

Figure 3.17. A = MORB normalized incompatible element diagram for group FRS eclogites. Normalizing values from Pearce and Parkinson (1993). B = Incompatible element diagram for low-K tholeiite (LKT) and calc-alkaline basaltic andesite (CAB) from an oceanic arc setting (Pearce et al., 1995).

3.6 Conclusions

Protoliths of eclogites from Stewart Lake are derived from an oceanic island-arc setting and can be divided into two types, calc-alkaline basalts, group SLC and low-potassium tholeiites, group SLK. The samples with calc-alkaline protoliths are more andesitic than the remaining samples from Stewart Lake. Group FRS eclogites from Faro, Ross River and Simpson Range are normal MORB or ocean floor basalts of tholeiitic character. Within-plate affinity is displayed by group BSR and includes PE-80-F3 from Faro.

Chapter 4 Sm-Nd Systematics and Geochemistry

4.1 Introduction

Samarium and neodymium are rare earth elements joined in a parent-daughter relationship by radioactive decay of ^{147}Sm to ^{143}Nd (Faure, 1986). The elements are widely distributed in common rocks and minerals and Sm-Nd is a useful dating tool for mafic igneous and metamorphic rocks. Nd isotopic composition also varies with tectonic origin of the rock as do the immobile trace elements commonly used as tectonic discriminators, such as Ti, Zr, Nb, V and Y. In this chapter, the results of Nd geochronology and Nd whole rock geochemistry are reported.

4.2 Whole Rock Model Ages

The "epsilon parameter" was introduced by DePaolo and Wasserburg (197 6) to compare the $^{143}Nd/^{144}Nd$ ratios of igneous and metamorphic rocks with CHUR or "chondritic uniform reservoir" at the present or at any time in the past. Positive epsilon

values indicate that the rocks crystallized from the residual solids after magma withdrawal and these rocks are depleted in the large ion lithophile (LIL) elements. Negative epsilon values indicate rocks were derived from or assimilated older crustal rocks whose whole rock Sm-Nd ratios were lowered by separation from CHUR (Faure, 1986). Although, CHUR can be used to calculate the date at which Nd in a crustal rock could have separated from the chondritic reservoir, these dates are geologically significant only when Sm-Nd ratios have not altered since separation from CHUR. Instead of employing CHUR, model dates are typically calculated relative to a depleted reservoir whose Sm-Nd ratio was increased by the formation of a partial melt during a previous episode of magma formation (Faure, 1986). This model depleted reservoir (or depleted mantle) is assumed to have a present-day $^{143}Nd/^{144}Nd$ ratio of 0.513163 and a $^{147}Sm/^{144}Nd$ ratio of 0.2137 (Faure, 1986).

The current $^{147}Sm/^{144}Nd$ and $^{143}Nd/^{144}Nd$ ratios for the eclogites can be used to calculate a depleted mantle model age which represents the maximum age of formation for the basaltic protolith. Whole rock model Nd ages have been calculated for 8 of the eclogite samples. These ages can be used as a guide to the maximum crystallization age of the protolith. Rocks with ratios too close to the values for the model depleted mantle

values are considered less geologically significant than those with ratios substantially different from those of the model. If the ratio is too close to the model value the lines will not intersect or the resulting model age will be too young or too old. Model ages for three of the eclogites are graphically represented on figure 4.1. The dash-dotted lines above and below the depleted mantle line represent model values assuming one epsilon unit error or more depleted or enriched sources.

The depleted mantle model age for sample PE-80-F2 (group FRS) is 160 Ma. This date is younger than the calculated Sm-Nd date for high-pressure metamorphism (e.g. 281 ± 15 Ma, PE-80-F1) and indicates that this rock was derived from an enriched source compared to the model reservoir. The maximum date of crystallization is 490 Ma when calculated relative to the lower dash-dotted line which assumes a more enriched source (model - 1 epsilon unit).

The protolith of sample PE-85-17 (group SLK) is a very depleted volcanic-arc rock. The model age for this rock is 360 Ma. Comparison of this model age with the date of high-pressure metamorphism of ~ 345 Ma indicates that metamorphism may have occurred relatively soon after formation of the protolith.

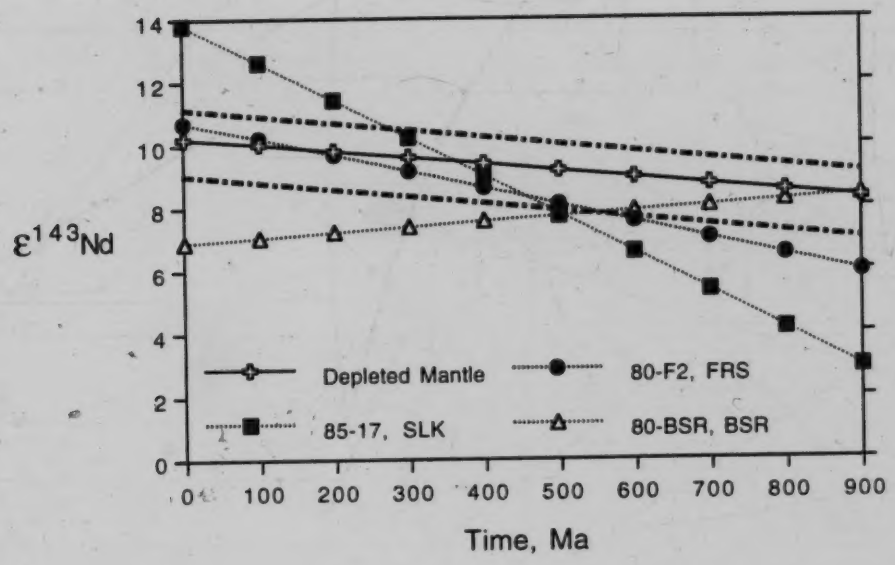

Figure 4.1. Plot showing evolution of $\varepsilon^{143}Nd$ over time (Ma) for selected eclogite samples. Depleted mantle model age shown by intersection of $\varepsilon^{143}Nd$ line with depleted mantle line. Depleted mantle values from Goldstein et al. (1989). Dash-dotted lines represent one $\varepsilon^{143}Nd$ unit of error (above depleted mantle line = greater depletion, below depleted mantle line = greater enrichment).

Sample PE-80-BSR originated as a within-plate basalt enriched in the LREEs and as such evolved from a source more enriched than the model depleted mantle. The calculated model age is 880 Ma. However, assuming a more enriched source (lower dash-dotted line; model - 1 epsilon unit) appropiate for the geochemistry, the maximum age of crystallization of the protolith is 600 Ma.

In summary, all the samples have positive epsilon values and have maximum model ages that are Late Precambrian or Phanerozoic. These model ages are very model dependent and are intended only to be a guide to the maximum crystallization dates.

4.3 Whole Rock Nd Geochemistry

The contents of immobile trace elements such as Ti, Zr, Nb and Y vary systematically with tectonic setting (Pearce and Norry, 1979) and are useful as tectonic discriminators. The eclogites examined in this study were divided into 4 groups on the basis of tectonic origin of their protoliths using immobile trace and rare earth elements. Plots of Ti, Zr, Nb and V against epsilon ^{143}Nd calculated at the time of metamorphism (~ 275 Ma for group FRS eclogites and ~ 345 Ma for groups SLC and SLK)

(figures 4.2-4.3) supports the division of the eclogites into the 4 distinct groups.

The samples from Stewart Lake (groups SLC and SLK) have low levels of Ti, Zr, Nb and V typical of oceanic island-arc rocks. However the SLC group of eclogites (calc-alkaline island-arc) have much lower epsilon Nd values than group SLK (low-K tholeiites). Nd is added from the slab as part of calc-alkaline enrichment trend. Eclogites of group FRS cluster on these plots with values characteristic of typical Phanerozoic mid-ocean ridge basalts with epsilon Nd of ~ 8-10 higher than group SLC but lower than group SLK. Group BSR also plots together and displays values common to within-plate basalts such as high Ti, Zr and Nb with low epsilon Nd.

4.4 Sm-Nd Geochronology

One objective of this study was to determine the age of high pressure metamorphism of the eclogites using Sm-Nd geochronology. Mafic and ultramafic igneous rocks have higher Sm-Nd ratios than rocks of felsic to intermediate composition and are datable by means of whole rock and/or internal mineral isochrons (Faure, 1986).

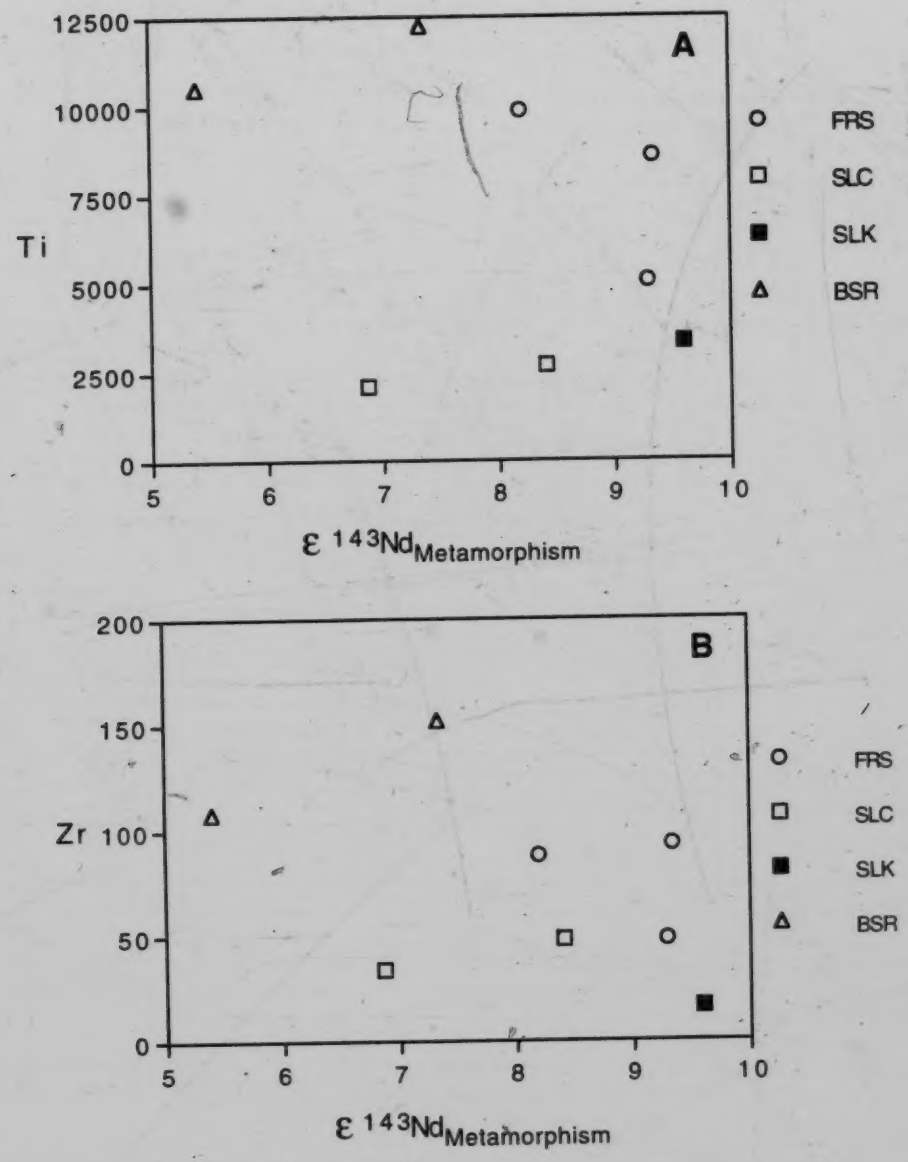

Figure 4.2. A = Ti versus $\varepsilon^{143}Nd_{Metamorphism}$ for Yukon-Tanana terrane eclogites. Time of formation calculated as 350 Ma for groups SLC and SLK and as 275 Ma for groups FRS and BSR. B = Zr versus $\varepsilon^{143}Nd_{Metamorphism}$ for Yukon-Tanana terrane eclogites.

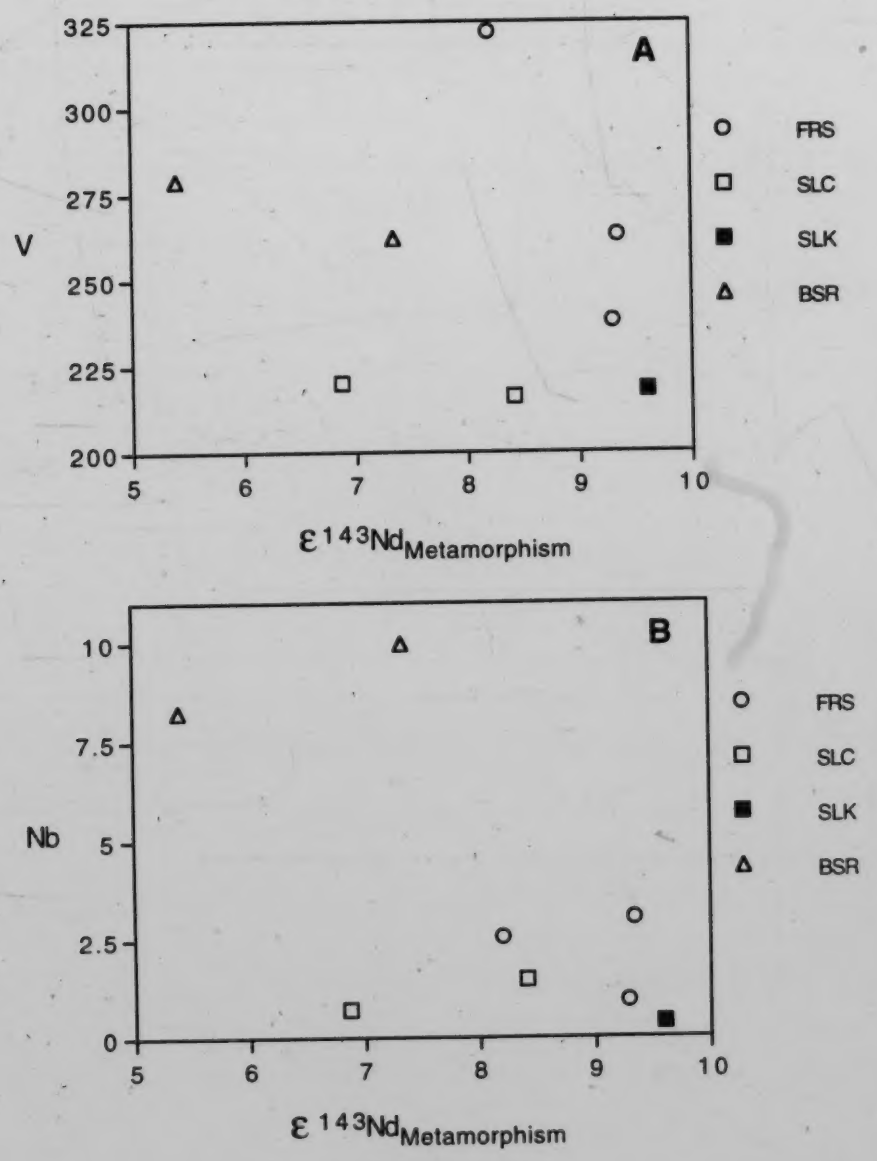

Figure 4.3. A = V versus $\varepsilon\ ^{143}Nd_{Metamorphism}$ for Yukon-Tanana terrane eclogites. Time of formation calculated as 350 Ma for groups SLC and SLK and as 275 Ma for groups FRS and BSR. B = Nb versus $\varepsilon\ ^{143}Nd_{Metamorphism}$ for Yukon-Tanana terrane eclogites.

The use of Sm-Nd, particularly employing garnet-clinopyroxene pairs, is very reliable for dating (Griffin and Brueckner, 1980; Sanders et al., 1984; Mørk and Mearns, 1986; Mørk et al., 1988; Paquette et al., 1989; Thöni and Jagoutz, 1992; Miller and Thöni, 1995). Griffin and Brueckner (1980) dated garnet and clinopyroxene pairs from several Norwegian country-rock eclogites to determine the age of high-pressure metamorphism. The resulting date of ~ 425 Ma is consistent with a previously reported U-Pb zircon date of 400-418 Ma for another Norwegian eclogites. The authors also confirmed the existence of several different protoliths for the eclogites by comparing Nd and Sr data. Sanders et al. (1984) employed the Sm-Nd isotopic system to date the Glenelg eclogite in north-west Scotland. The eclogite was assumed to be "probably" Proterozoic but previously obtained K-Ar dates are considered unreliable due to the presence of excess argon (Sanders et al. ,1984). The 1082 ± 24 Ma Sm-Nd date provides strong evidence of Grenville age eclogite metamorphism. Miller and Thöni (1995) employed both Sm-Nd and Rb-Sr isotope systematics in combination with geochemistry to determine the origin and age of eclogite protoliths and timing of eclogite metamorphism in the Austrian Alps. The results indicated the gabbro and basaltic protoliths experienced three phases of

metamorphism prior to transformation into eclogites at ~ 370-340 Ma with peak pressures between 360 and 350 Ma.

Reconnaissance work in eclogite-facies terranes is typically conducted using t he K-Ar and $^{40}Ar/^{39}Ar$ methods. In these high-pressure rocks, excess Ar problems can result in meaningless dates (Vidal and Hunziker, 1985). Most eclogites have been overprinted by later amphibolite and greenschist facies metamorphism and can contain multiple phases of minerals which increases the uncertainty of dates obtained by the K-Ar and $^{40}Ar/^{39}Ar$ systems. K-Ar and $^{40}Ar/^{39}Ar$ dates are cooling dates and therefore provide a minimum age of high-pressure metamorphism.

The Rb-Sr method is generally not u sed on eclogites because of their low Rb-Sr ratios (Faure, 1986). The low Rb contents of the mafic protoliths also poses a problem, as a small change in Rb content during metamorphism can significantly alter the Rb-Sr system in an eclogite (Vidal and Hunziker, 1985). Sr is considered to be highly mobile during metamorphism and also effects the Rb-Sr ratios.

Unlike K-Ar and Rb-Sr, Sm-Nd is usually unaffected by metamorphism and Sm and Nd are effectively fractionated between garnet and clinopyroxene. In addition they are very similar in crystal-chemical behaviour (Griffin and Brueckner, 1980; Sanders et al.,

1984). The minerals within eclogites display very different REE patterns (Vidal and Hunziker, 1985). Garnet is usually more LREE depleted and HREE enriched than coexisting clinopyroxene. As a result significant differences in $^{143}Nd/^{144}Nd$ ratios can develop relatively quickly allowing good precision for Sm-Nd mineral dates. Nd also stops diffusing at temperatures close to eclogite metamorphic conditions providing the age of high-pressure metamorphism rather than cooling ages (Vidal and Hunziker, 1985).

Whole rock and garnet and clinopyroxene mineral separates were analyzed for Sm-Nd isotopes for several of the eclogites (Table 7). The analysis of sample PE-80-F1 (Faro, group FRS), using a combination of whole rock and mineral separate data results in an isochron date of 281 ± 15 Ma (figure 4.4) for high-pressure metamorphism (M.S.W.D. = 7.06). An ideal value for M.S.W.D. is 1.0. The M.S.W.D. value obtained for this analysis and the one reported below reflects the dificulty in analysing samples with Sm close to the detection limit.

The second sample to be dated using the Sm-Nd system for whole rock and mineral separate data is PE-85-21 (Ross River, group FRS). The analysis resulted in an isochron date of 255 ± 8.1 Ma (figure 4.5), (M.S.W.D. of 13.5). Garnets from this sample proved to be the most difficult to dissolve. In each case the age was calculated

Table 7

Whole Rock Sm-Nd Data

Sample	**PE-80-F1**	**PE-80-F2**	**PE-80-F3**	**PE-80-BSR**	**PE-85-10**	**PE-85-11-1**	**PE-85-17**	**PE-85-21-7**
Location	Faro	Faro	Faro	Last Peak	Stewart Lake	Stewart Lake	Stewart Lake	Ross River
Sm ppm	2.30	1.72	2.46	5.87	1.06	1.92	0.83	3.99
Nd ppm	6.28	4.35	8.59	19.30	3.28	6.05	1.73	11.71
147Sm/144 Nd	0.22148	0.23847	0.17296	0.18393	0.19510	0.19237	0.29146	0.20604
143Nd/144Nd	0.513161	0.513189	0.512872	0.512991	0.512986	0.513059	0.513347	0.513075
2 sigma mean	0.000010	0.000011	0.000009	0.000007	0.000011	0.000007	0.000009	0.000008
Epsilon Nd @ 275 Ma	9.3	9.3	5.4	7.3	6.9	8.4	9.7	8.2
TDM (Goldstein) Ga	-0.04	0.16	1.09	0.88	1.45	0.74	0.36	1.75

Mineral Separate Sm-Nd Data

Sample	**80-F1-g1**	**80-F1-px**	**80-F1-g2**	**80-F1-g1A**	**80-F1-g1B**	**85-21-p1**	**85-21-g1**	**85-21-g2**	**85-21-g1A**	**85-21-g2A**
mineral type	gaarnet	pyroxene	garnet	garnet	garnet	pyroxene	garnet	garnet	garnet	garnet
Location	Faro	Faro	Faro	Faro	Faro	Ross River	Ross River	Ross River	Ross River	Ross River
Sm ppm	1.33	1.67	1.16	1.32	1.32	1.76	2.03	2.05	2.11	2.06
Nd ppm	1.57	4.57	1.01	1.54	1.54	5.52	0.80	0.86	0.81	0.82
147Sm/144 Nd	0.51280	0.22165	0.69646	0.51857	0.52051	0.19295	1.54231	1.43511	1.57335	1.51223
143Nd/144Nd	0.513679	0.513149	0.514044	0.513678	0.513703	0.513053	0.515274	0.515164	0.515369	0.515221
2 sigma mean	0.000010	0.000011	0.000036	0.000014	0.000048	0.000007	0.000026	0.000025	0.000039	0.000065
Epsilon Nd @ 275 Ma	9.2	9.1	9.9	9.0	9.4	8.2	4.2	5.8	4.9	4.2
TDM (Goldstein) Ga	0.26	-0.27	0.28	0.26	0.27	0.81	0.24	0.25	0.25	0.24

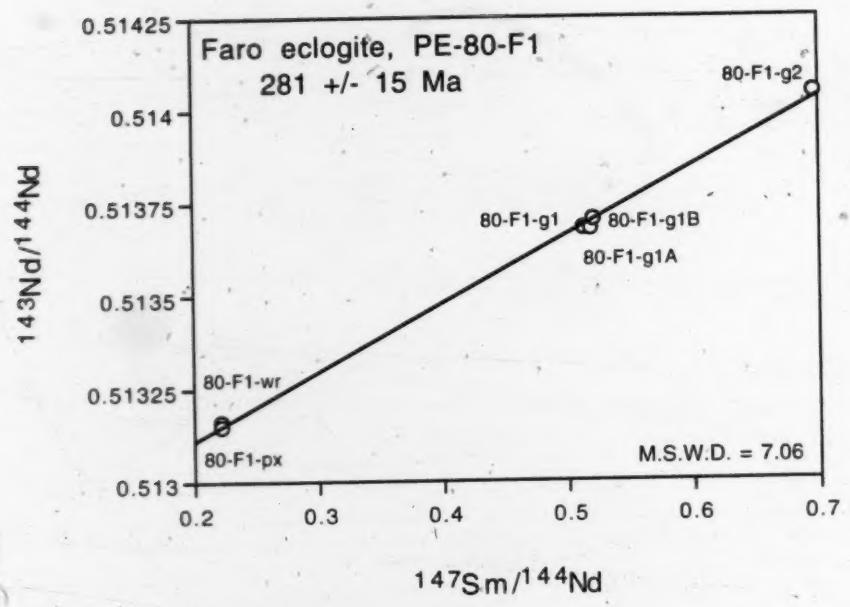

Figure 4.4. Sm-Nd isochron based on whole rock and garnet and pyroxene mineral separates for Faro eclogite PE-80-F1.

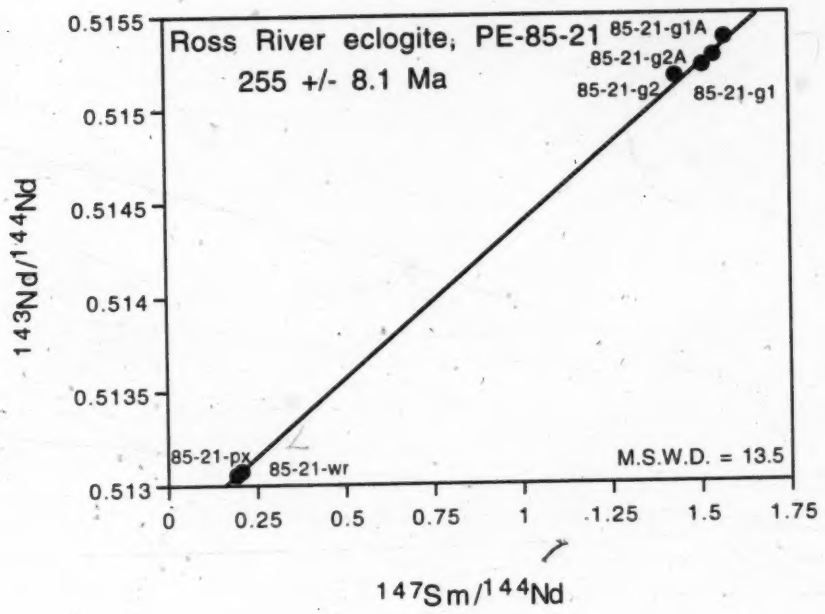

Figure 4.5. Sm-Nd isochron based on whole rock and garnet and pyroxene mineral separates for Ross River eclogite PE-85-21.

using a model 3 Yorkfit which assumes scatter is due to analytical error plus normal-distribution of error in initial $^{143}Nd/^{144}Nd$. The results of the study indicate that true closed system behavior may not have been obtained by the garnets during high-pressure metamorphism because there is some scatter about the isochrons. Garnet fractions with differing grain sizes have slightly different isotopic ratios indicating limited open system behavior on the sub-grain size level.

Sample PE-85-17 (Stewart Lake, group SLK) was analyzed for both Sm-Nd and Rb-Sr but provided no useful data. The eclogite is strongly sheared and retrograde metamorphic minerals are evident. It appears the Rb-Sr system was affected by metamorphism and the garnet and clinopyroxene pairs did not form at the same time or were affected by the later metamorphism and shearing rendering them undatable using the Sm-Nd system.

Chapter 5 Discussion and Conclusions

5.1 Summary of Results

Based on the analysis of major, trace and rare earth element geochemistry, eclogites from Faro, Ross River, Last Peak, Simpson Range and Stewart Lake areas of the YTT can be subdivided into four distinct groups. Eclogites from Faro, Ross River, Simpson Range and one from Stewart Lake (PE-85-16B) are derived from normal mid-ocean ridge basalts (MORB) (group FRS). Last Peak eclogites and one sample from Faro (PE-80-F3) have a within-plate basaltic protolith (group BSR). The remaining samples from Stewart Lake share oceanic-island arc affinity but can be further separated into two groups; one displaying calc-alkaline basaltic-andesite characteristics (higher SiO_2) (group SLC) and the other low-potassium tholeiitic characteristics (group SLK). Sm-Nd dating of two eclogites resulted in dates of 281 ± 15 Ma for Faro and 255 ± 8.1 Ma for Ross River. ε_{Nd} model ages for these eclogites provide approximate maximum ages of formation for the protoliths. The ε_{Nd} model age for eclogite from Faro is 490 Ma, 600 Ma for Last Peak and 360 Ma for Stewart Lake. The results of the geochemical and

Sm-Nd isotopic studies have important implications for the various tectonic models proposed for the TTZ and the YTT.

5.2 Discussion

5.2.1 Geochemical and Age Correlations

The results of this study, together with recent $^{40}Ar/^{39}Ar$ dating (Erdmer et al., in press) support the hypothesis that two separate phases of subduction and arc activity are preserved in the YTT (Mortensen, 1992). Geochemically, eclogites from the Stewart Lake area show clear island-arc affinities and as such may represent the mafic components of the Mississippian arc system identified elsewhere in the YTT (e.g., Stevens et al., 1996; Grant, 1997). $^{40}Ar/^{39}Ar$ mica cooling dates for these rocks are 346 ± 3 Ma (PE-85-17; Erdmer et al., in press) and are interpreted to be the true cooling ages. The ε_{Nd} model age for a Stewart Lake eclogite (PE-85-17) is 360 Ma, which indicates the eclogite protolith must also be Paleozoic. An integrated $^{40}Ar/^{39}Ar$ mica cooling date of 218 ± 1 Ma (PE-85-10; Erdmer et al., in press) for one Stewart Lake sample is problematic, because it is only 2 km away from the other dated Stewart Lake eclogite. Both samples

have oceanic island-arc affinities but may not record the same subduction event. Alternatively, the dates may reflect different exhumation times (Erdmer et al., in press) or may indicate that the isotopic systems were partially reset during accretion to the North American continental margin. The date is based on 37% gas released and does appear to have an older component and therefore may not be a true age.

Eclogites with mid-ocean ridge basalt characteristics are also found at Stewart Lake and Simpson Range, the latter of which has a similar cooling date as the Stewart Lake samples. Erdmer et al. (in press) report an integrated $^{40}Ar/^{39}Ar$ mica cooling date of 346 ± 1 Ma for Simpson Range eclogite. The MORB-like rocks may represent subducted ocean floor or back-arc basin material associated with the Mississippian age volcanic arc.

The second age of subduction and arc magmatism preserved in YTT rock s occurred in the Permian. Eclogites in the Faro, Ross River and Last Peak areas appear to record this subduction event. The protolith for most eclogites at Faro and Ross River is n-MORB and may indicate these rocks represent subducted ocean floor or rocks from a back-arc basin related to the Permian subduction system. The relatively old ε_{Nd} model age for Faro (490 Ma) does not exclude either possibility.

Based on the within-plate affinity of the Last Peak eclogites and a Faro sample (PE-80-F3), these rocks may represent basaltic dyke rocks of continental character which were metamorphosed as part of the trench mélange in the subduction zone. The within-plate rocks are currently hosted by Nisutlin assemblage rocks; a dominantly continental package of metasediments (Stevens et al., 1996). Stevens et al. (1996) state that the Nisutlin assemblage acted as a coherent body during Permian age subduction. As a result, high-pressure metamorphism was concentrated along the edge of the block and did not affect the large portions of the assemblage or that metamorphism did not obliterate primary depositional and intrusive relationships. The presence of eclogite with a within-plate protolith may indicate that more of the assemblage experienced high-pressure metamorphism than proposed by Stevens et al. (1996) or may represent dyke rocks intruded into the edge of the Nisutlin crustal block before or during the onset of subduction.

Faro and Ross River record high-pressure metamorphism at 281 ± 15 Ma and 255 ± 8.1 Ma, respectively. Although the Ross River is younger than the Faro date, they are nearly within error of each other. It shows that rocks at Ross River experienced peak

high-pressure metamorphic conditions slightly later than at Faro. U-Pb zircon dating of an eclogite from Last Peak results in an date of 269 ± 2 Ma (Creaser et al., 1997a). A U-Pb zircon date of 265.7 ± 6 Ma (K. Fallas, 1997, personal communication) is recorded by eclogite from the St. Cyr klippe. These ages are consistent and indicate that high-pressure metamorphism may have peaked in the Early Permian. $^{40}Ar/^{39}Ar$ cooling dates for Faro and Ross River eclogites (Erdmer et al., in press) suggest that these rocks cooled by or before 261 Ma. An $^{40}Ar/^{39}Ar$ mica cooling date of 239 ± 1 Ma for Last Peak eclogite is younger than the U-Pb zircon age and may represent later exhumation (Erdmer et al., in press).

5.2.2 Relationship to Slide Mountain

The Slide Mountain terrane is an oceanic sequence of basalt, gabbro and sedimentary rocks interpreted to have formed in a Late Paleozoic-Early Mesozoic marginal basin of the North American continental margin (Roback et al., 1994). Previous tectonic models for the origin of the YTT have correlated all metamorphosed mafic igneous rocks in the terrane, including the Anvil assemblage of the TTZ, with the Slide

Mountain terrane (Hansen, 1990; Hansen et al., 1991; Wheeler et al., 1991). Geochemical studies of basalt from the Kaslo Group and the Fennel Formation by Roback et al (1994) and Smith and Lambert (1995) document strong similarities between Slide Mountain basalts and n-MORBs. Creaser et al. (1997b) reported that Anvil greenstones from the TTZ appear most similar to calc-alkaline basalts formed at active continental margins, and suggest that the correlation of Anvil assemblage rocks with Slide Mountain terrane is incorrect based on the marked differences of basalt type. They suggest the tectonic models need to be revised to reflect this disparity. The Stewart Lake eclogites are hosted by rocks of the Anvil assemblage (Erdmer, 1987) and display calc-alkaline or low-potassium tholeiitic island arc character. The Anvil assemblage rocks are correlated with Slide Mountain terrane by Erdmer et al. (in press). Eclogites from Stewart Lake with calc-alkaline character could represent the more metamorphosed equivalents of the Anvil assemblage basalts and gabbros seen in the TTZ and elsewhere in the YTT.

Eclogites from Faro, Ross River, Simpson Range and one Stewart Lake sample have n-MORB protoliths. A comparison of rare earth element patterns for eclogites from Faro, Ross River and Simpson Range with those of metabasalts from the Kaslo Group and the Fennel Formation (figure 5.1) shows striking similarities between the

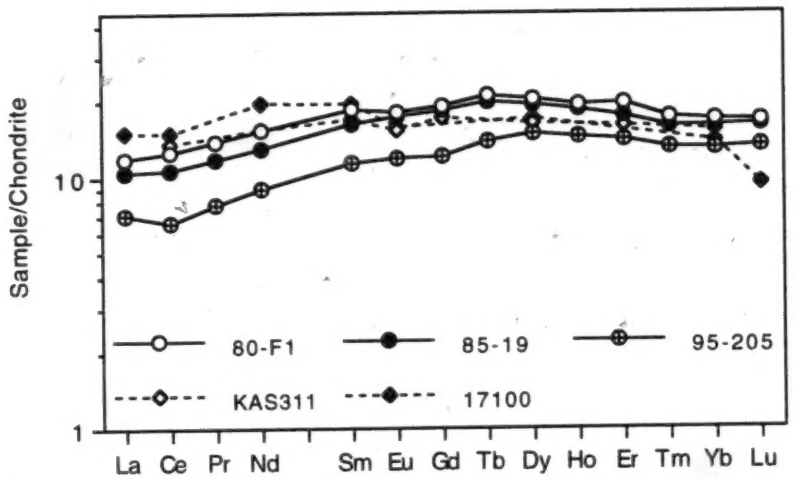

Figure 5.1. REE diagram for selected Faro, Ross River and Simpson Range eclogites. Shown for comparison are Paleozoic metabasalts from the Kaslo Group and the Fennel Formation of the Slide Mountain terrane (Roback et al., 1994; Smith and Lambert, 1995). Normalizing values from Newpet (1994) (La; 0.3290, Ce; 0.8650, Pr; 0.1300, Nd; 0.6300, Sm; 0.2030, Eu; 0.0770, Gd; 0.2760, Tb; 0.0498, Dy; 0.3430, Ho; 0.0770, Er; 0.2250, Tm; 0.0352, Yb; 0.2200, Lu; 0.0339).

Yukon-Tanana and Slide Mountain terrane rocks. The older Simpson Range eclogite is more depleted than the other samples and is also known to be older than the Slide Mountain terrane rocks. A similar comparison of incompatible element patterns (figure 5.2) also displays similarities between Slide Mountain rocks and those of Faro, Ross River and to a lesser extent Simpson Range. The metabasalts of Slide Mountain are more enriched in Nb and Zr but the overall pattern is comparable. These similarities may reflect a correlation between some eclogites with n-MORB protoliths from the YTT and Slide Mountain basalts as suggested by the tectonic models. This provides further evidence that the correlation of Anvil assemblage rocks and eclogites at Stewart Lake with Slide Mountain basalts needs to be revised.

The tectonic relationship of Anvil assemblage rocks with those of Slide Mountain terrane needs to be examined in more detail because current explanations for their positions are not adequate based on their differing character. The juxtaposition of normal mid-ocean ridge basalt and continental within-plate basalt at Faro also calls into question the grouping together of all eclogites found in the YTT. Current tectonic models do not consider the possible differences in protolith demonstrated by the eclogites and do not address how eclogites of differing protoliths are emplaced in close proximity. Further

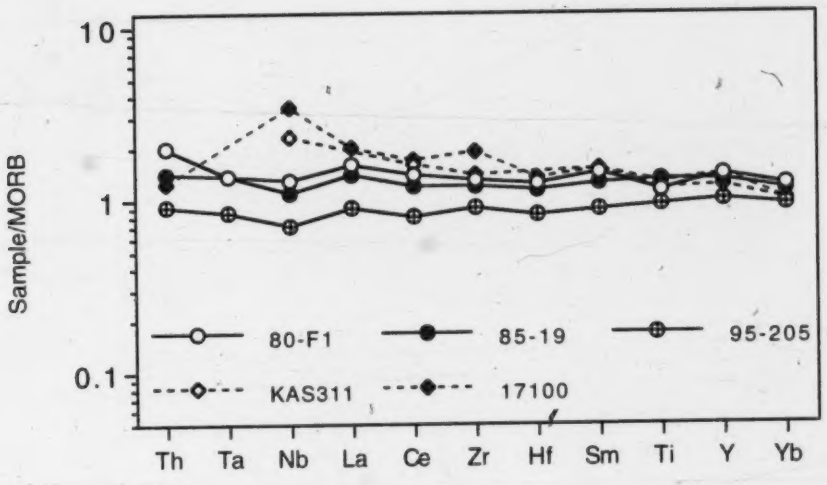

Figure 5.2. Incompatible element diagram for selected Faro, Ross River and Simpson Range eclogites. Shown for comparison are Paleozoic metabasalts from the Kaslo Group and the Fennel Formation of Slide Mountain terrane (Roback et al., 1994; Smith and Lambert, 1995). Normalizing values from Pearce and Parkinson (1993).

geochemical work needs to be done on the rocks with a basaltic nature or with basaltic protoliths to determine correct terrane assignments. Detailed structural analysis is also required to explain the possibility of more complex shuffling of the eclogites and their host rocks than was previously thought.

5.2.3 Constraints for Tectonic Models

Tempelman-Kluit (1979) proposed the first tectonic model for the TTZ and the YTT, in which the TTZ was part of a subduction complex that developed on the North American continental margin during the Late Paleozoic-Early Mesozoic. The floor of the Anvil Ocean (Slide Mountain Ocean, c.f. Stevens et al., 1996) was subducted beneath North America and resulted in the collision of the Lewes River arc (Stikinia) with North America and the obduction of the subduction complex onto the continental margin. This model was modified by Erdmer and Helmstaedt (1983) and Erdmer (1985, 1986 and 1992) with examination of eclogites and blueschist from the TTZ suggesting that rocks of the zone record a range of pressure-temperature and strain conditions interpreted to reflect nearly all levels of the subduction and collision zone.

The initial model of Tempelman-Kluit (1979) was further modified by Mortensen and Jilson (1985) and Mortensen (1992). The authors interpreted the Devonian to Mississippian orthogneiss as the product of subduction and arc magmatism unrelated to the second episode of subduction in the Permian, indicating that two phases of subduction are preserved within the TTZ. The authors also concluded that the terrane evolved as a coherent package rather than as trench mélange. Later work by Stevens et al. (1996) confirmed the volcanic arc affinity of the orthogneiss and concluded that the Nisutlin assemblage evolved as a coherent crustal block based on its internal stratigraphy. The authors also show that both the Nisutlin and Anvil assemblages are >350 Ma.

Hansen (1987, 1989, 1992a and 1992b) and Hansen et al. (1989, 1991) supported the model proposed by Tempelman-Kluit (1979) with some modifications and greater emphasis placed on the subduction-zone processes. Hansen (1987, 1992a and 1992b) suggested continuous oblique subduction and high-pressure metamorphism for the Teslin Tectonic rocks from the Permian until Late Triassic or Early Jurassic time. Rocks of the TTZ are interpreted as rocks scraped off the subducting slab with high-pressure metamorphic conditions and ductile deformation attributed to backflow, margin-parallel flow and downflow within the west-dipping subduction channel. Eclogites associated

with the Permian subduction event have both n-MORB and within-plate protoliths. The presence of diverse rock types indicates both subducting ocean floor and portions of the Nisutlin and/or Anvil assemblages were also metamorphosed and later exhumed in addition to material scraped off the slab.

Based on the $^{40}Ar/^{39}Ar$ muscovite dates for Stewart Lake and Simpson Range eclogites and the depleted mantle model age for Stewart Lake, these rocks are likely related to the Mississippian subduction event recorded by rocks in other areas of the YTT. These rocks were not affected by the final accretion of the terrane to the North American continental margin, with one possible (Triassic age) exception. Contrary to the model proposed by Tempelman-Kluit, this indicates subduction was not continuous from the Late Paleozoic-Early Mesozoic.

New $^{40}Ar/^{39}Ar$ muscovite dates of 270-260 Ma from Yukon-Tanana eclogites and a blueschist suggests that muscovite was not isotopically reset during the accretion of the high-pressure rocks to North America (Creaser et al., 1997a). A separate tectonic event occurred in the Late Triassic to Early Jurassic and is characterized by abundant calc-alkaline magmatism in the YTT and the western accreted terranes and may be associated with the final assembly of the Intermontane Belt (Mortensen, 1992). A broad

range of eclogite $^{40}Ar/^{39}Ar$ mica dates and U-Pb dates of subduction related magmatism would be expected by tectonic models that suggest subduction beginning in the Permian continued until the early Mesozoic. The restricted range and similarity of regional eclogite $^{40}Ar/^{39}Ar$ mica dates (Erdmer et al., 1996, 1997, in press), U-Pb eclogite metamorphic date (Creaser et al., 1997a, K. Fallas, 1997, personal communication), U-Pb dates of calc-alkaline rocks (Mortensen, 1992) and eclogite Sm-Nd dates of high-pressure metamorphism support the concept of a short-lived subduction event in the Permian, followed by a change in the tectonic regime until the Late Triassic (Mortensen, 1992; Creaser et al., 1997a). The existence of two "separate" subduction events, one Mississippian in age and the other Permian in age, is also supported by the results of this study and previous dating of eclogites from the YTT.

Keijzer and Williams (1997) examined the metamorphic field gradient in the Yukon-Tanana in order to establish the direction of subduction-zone polarity. As a result of their field and structural studies they concluded that a subduction zone argument is not valid for high- grade metamorphic rocks in the TTZ. The authors indicate that the rocks are preserved in an overturned limb of a large scale fold structure. The results of the

present study appear to contradict their argument, as the eclogites are type C indicating metamorphism in a subduction zone rather than at great depths on the continent.

An examination of tectonic model prop osed by Stevens et al. (1996) (figure 5.3) and the results of this study indicate that only minor revisions of the model are neceesary to accomodate the new data. The eclogites from Last Peak and Faro with continental within-plate affinity could have intruded the margin of the Nisutlin/Anvil block in either the Mississippian or the Permian stages. They are hosted by Nisutlin metasedimentary rocks and the model ages of these rocks do not exclude either possibility. Based on the age of high-pressure metamorphism and their geochemistry, the remaining Faro and Ross River eclogites may preserve subducted ocean floor of the Slide Mountain Ocean. At Faro, eclogites with both within-plate and n-MORB characteristics are present. If the Faro eclogites with MORB protoliths are associated with Slide Mountain terrane, complex tectonic interleaving must have taken place, which is not supported by the field evidence. Erdmer et al. (in press) states that the Faro, Ross River and Last Peak eclogites are in pre-metamorphic contact with their host Nisutlin rocks. Therefore the eclogites with MORB (group FRS) and continental within-plate protoliths (group BSR) probably belong to the same terrane. The juxtaposition of basalts with very different protoliths

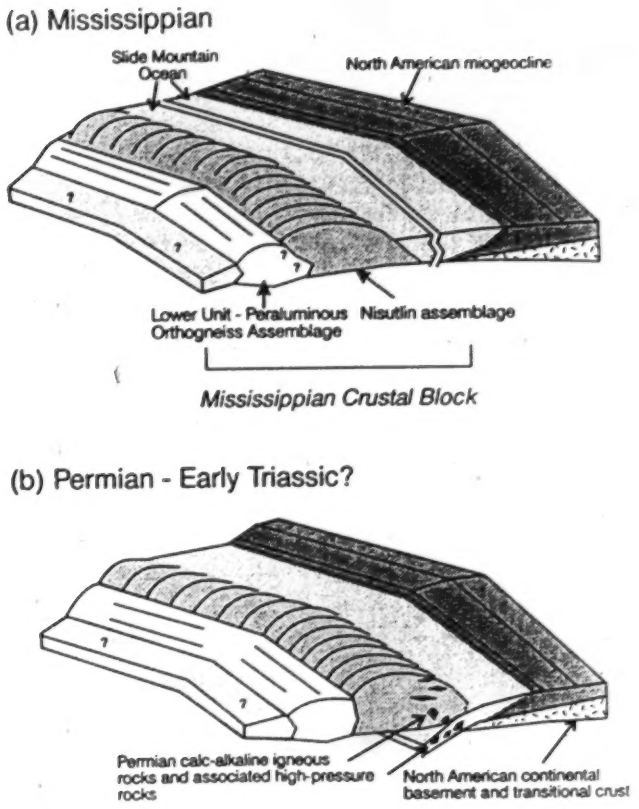

Figure 5.3. Model for the Paleozoic evolution of the Nisutlin assemblage in the Teslin tectonic zone. (a) Mississippian: The Nisutlin assemblage is part of a crustal block at the distal edge of the North American continental margin. (b) Permian - EarlyTriassic?: The Nisutlin assemblage lies in the hanging-wall of a late Paleozoic and early Mesozoic west-dipping subduction zone that closed the Slide Mountain Ocean. (from Stevens et al., 1996)

could have been produced during the initial stages of rifting in the back arc between the Nisutlin/Anvil block and the continental margin of North America. The first basalts produced would likely intrude the block as mafic dykes and as rifting continued the basalts produced would become more depleted and MORB-like. These rocks were subducted beneath North America, metamorphosed and later exhumed as eclogites.

A modified tectonic model is proposed based on the results of this study. Prior to 350 Ma, the Nisutlin and/or Anvil assemblages were located at a distal position relative to the North American continental margin. The initiation of east-facing subduction (Creaser et al., 1997b) in the Mississippian produced calc-alkaline magmatism and resulted in the underplating of primitive oceanic island-arc and ocean floor material eclogites beneath the Nisutlin/Anvil hanging-wall block (figure 5.4). The basaltic protoliths for eclogites from Stewart Lake and Simpson Range areas experienced high-pressure metamorphism during this period of subduction. Cooling ages for the eclogites indicate that rocks were exhumed by ~345 Ma. Formation of the Slide Mountain Ocean followed by back arc spreading separated the Nisutlin/Anvil block from the North American continental margin. A second phase of calc-alkaline magmatism occurred in the Mid-Permian when rocks from the Slide Mountain Ocean were subducted westward under North America.

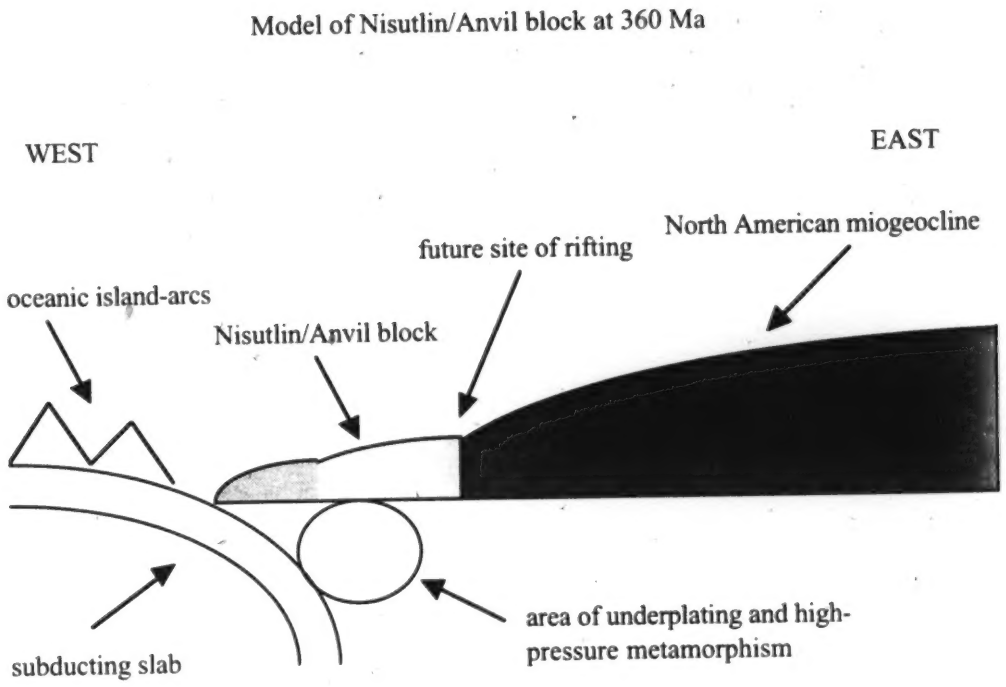

Figure 5.4. Model of the Nisutlin/Anvil block and the North American continental margin at ~ 360 Ma. The paleo-Pacific ocean floor is being subducted at an east-dipping subuction zone. Oceanic island arc material is also being subducted and also underplated to the hanging-wall of the Nisutlin/Anvil block. The island arc and ocean floor material form the protoliths of the Stewart Lake and Simpson Range eclogites..

The protoliths for the Last Peak and Faro eclogite intruded the crustal margin of the Nisutlin/Anvil block. No new oceanic-arc rocks formed but continental arc rocks are represented by the 270 Ma plutonism. Peak high-pressure metamorphism in the subduction zone occurred between ~275 and ~269 Ma. The subduction event was short-lived and the tectonic regime changed until the onset of magmatism in the Late Triassic to Early Jurassic. This event probably represents the final accretion of the Yukon-Tanana terrane onto the North American continental margin, during which remnants of the floor of Slide Mountain Ocean, metamorphosed ocean floor (Faro and Ross River eclogites) and the Nisutlin and Anvil assemblages were obducted onto the continent.

5.3 Conclusions

1. Eclogites from Faro, Ross River, Simpson Range and one from Stewart Lake (group FRS) have mid-ocean ridge basaltic protoliths (MORB) based on their trace and rare earth element geochemistry.

2. Eclogites from Stewart Lake share oceanic island-arc affinity and can be further subdivided into two groups based on their trace and rare earth element geochemistry. One group displays calc-alkaline andesitic character (group SLC) and the other displays low-potassium tholeiitic character (group SLK).

3. Eclogites from Last Peak and one from Faro (group BSR) have continental within-plate basaltic protoliths based on their trace and rare earth element geochemistry.

4. Sm-Nd dating of a Faro eclogite (PE-80-F1), using whole rock and mineral separate data, resulted in an date of 281 ± 15 Ma. A Sm-Nd date of 255 ± 8.1 Ma was obtained from whole rock and mineral separate data for a Ross River eclogite (PE-85-21).

5. Two periods of subduction are recorded by eclogites within the YTT. Eclogites from Simpson range and Stewart Lake were metamorphosed during Mississippian age subduction based on their $^{40}Ar/^{39}Ar$ mica cooling dates (Erdmer et al., in press). The n-MORB and volcanic arc character of these rocks invites a correlation to the arc magmatism known throughout the YTT at this time. Faro, Ross River and Last Peak

eclogites were metamorphosed during a short-lived Permian age subduction event based on their Sm-Nd dates, $^{40}Ar/^{39}Ar$ mica cooling ages and U-Pb zircon dates.

6. The results of this study indicate that the eclogites in the YTT represent diverse tectonic settings and at least two phases of high-pressure metamorphism related to subduction zone processes. Current tectonic models need revision to accommodate the results provided by this study.

References

Brown, R.L., Carr, S.D., Harvey, J.L., Williams, P.F. and De Keijzer, M., 1995. Structure and significance of the Teslin suture zone. *in* Slave-Northern Cordillera Lithospheric Experiment (SNORCLE) Transect Meeting report no. **44**, Cook, F. and Erdmer, P., editors, p. 56-62.

Cairnes, D.D., 1914. The Yukon Alaska International boundary between Porcupine and Yukon Rivers. Memoirs of the Geological Survey of Canada, **67**, 161 pp.

Clark, D., 1994. Newpet for Dos. Memorial University of Newfoundland, Department of Earth Sciences, computer shareware program.

Coney, P.J., Jones, D.L.and Monger, J.W.H., 1980. Cordilleran suspect terranes. Nature, **288**, p. 329-333.

Creaser, R.A., Heaman, L.M., and Erdmer, P., 1997a. Timing of high-pressure metamorphism in the Yukon-Tanana terrane, Canadian Cordillera: constraints from U-Pb zircon dating of eclogite from the Teslin tectonic zone. Canadian Journal of Earth Sciences, **34**, p. 709-715.

Creaser, R.A., Erdmer, P, Stevens, R.A. and Grant, S.L., 1997b. Tectonic affinity of Nisutlin and Anvil assemblage strata from the Teslin tectonic zone, northern Canadian Cordillera: Constraints from neodymium isotope and geochemical evidence. Tectonics, **16**, p. 107-121.

deKeijer, M. and Williams, 1997. A new view on the structural framework of the Teslin zone, south-central Yukon. *in* Slave-Northern Cordillera Lithospheric Evolution (SNORCLE) Transect and Cordilleran Tectonics Workshop Meeting, Lithoprobe Report no. **56**, Cook,F and Erdmer, P. editors, p. 96-102.

DePaolo, D.J. and Wasserburg, G.J., 1976. Nd isotopic variations and petrogenetic models. Geophysical Res. Letters, **3**, p. 249-252.

Erdmer, P., 1985. An examination of the cataclastic fabrics and the structures of parts of Nisutlin, Anvil and Simpson allochthons, central Yukon: test of the arc-continent collision model. Journal of Structural Geology, **7**. p. 57-72.

Erdmer, P., 1987. Blueschist and eclogite in mylonitic allochthons, Ross River and Watson Lake areas, southeastern Yukon. Canadian Journal of Earth Sciences, **24**, p. 1439-1449.

Erdmer, P., 1992. Eclogitic rocks in the St Cyr klippe, Yukon, and their tectonic significance. Canadian Journal of Earth Sciences, **29**, p. 1296-1304.

Erdmer, P. and Armstrong, R.L., 1988. Permo-Triassic isotopic dates for blueschist, Ross River area, Yukon. *in* Yukon Geology, **2**, Exploration and Geological Services Division, Yukon, Indian and Northern Affairs Canada, p. 33-36.

Erdmer, P. and Helmstaedt, H., 1983. Eclogite from central Yukon: a record of subduction at the western margin of ancient North America. Canadian Journal of Earth Sciences, **20**, p. 1389-1408.

Erdmer, P., Ghent, E.D., Archibald, D.A. and Stout, M.Z., 1998. Paleozoic and Mesozoic high-pressure metamorphism at the margin of ancestral North America in central Yukon. Geological Society of America Bulletin, **in press**.

Faure, G., 1986. Principles of Isotope Geology. John Wiley and Sons, New York, 589 pp.

Gabrielse, H., Monger, J.W.H., Wheeler, J.O. and Yorath, C. J., 1991. Part A. Morphogeological belts, tectonic assemblages and terranes. *in* Chapter 2 of Geology of the Cordilleran Orogen in Canada, H. Gabrielse and C.J. Yorath, editors, Geological Survey of Canada, Geology of Canada, **no. 4**, p. 15-28. (also Geological Society of America, The Geology of North America, **v. G-2**).

Gabrielse, H. and Yorath, C. J., 1991. Tectonic Synthesis; Chapter 18. *in* Geology of the Cordilleran Orogen in Canada, H. Gabrielse and C.J. Yorath, editors, Geological Survey of Canada, Geology of Canada, **no. 4**, p. 677-705. (also Geological Society of America, The Geology of North America, **v. G-2**).

Grant, S. L., 1997. Geochemical, radiogenic tracer isotopic, and U-Pb geochronological studies of the Yukon-Tanana terrane rocks from the Money klippe, southeastern Yukon, Canda. Unpublished M.Sc. thesis, University of Alberta, 177 pp.

Goldstein, S.L., O'Nions, R.K. and Hamilton, P.J., 1984. A Sm-Nd isotopic study of atmospheric dusts and particulates from major river systems. Earth and Planetary Science Letters, **70**, p. 221-236.

Griffin, W.L. and Brueckner, H.K., 1980. Caledonian Sm-Nd ages and a crustal origin for Norwegian eclogites. Nature, **285**, p. 319-320.

Hansen, V.L., 1988. A model for terrane accretion: Yukon-Tanana and Slide Mountain Terranes, northwest North America. Tectonics, **7**, p. 1167-1177.

Hansen, V.L., 1989. Structural and kinematic evolution of the Teslin suture zone, Yukon: record of an ancient transpressional margin. Journal of Structural Geology, **11**, p. 717-733.

Hansen, V.L., 1990. Yukon-Tanana Terrane: a partial acquittal. Geology, **18**, p. 365-369.

Hansen, V.L., 1992a. Backflow and margin-parallel shear within an ancient subduction complex. Geology, **20**, p. 71-74.

Hansen, V.L., 1992b. P-T evolution of the Teslin suture zone and Cassiar tectonites, Yukon, Canada: evidence for A- and B-type subduction. Journal of Metamorphic Geology, **10**, p. 239-263.

Hansen, V.L., Mortensen, J.K. and Armstrong, R.L., 1989. U-Pb, Rb-Sr and K-Ar isotopic constraints for ductile deformation and related metamorphism in the Teslin suture zone, Yukon-Tanana terrane, south-central Yukon. Canadian Journal of Earth Sciences, **26**, p. 2224-2235.

Harker, A., 1904. The Tertiary igneous rocks of Skye. Memoirs of the Geological Survey of the United Kingdom, 481pp.

Hooper, P.R., Johnson, D.M. and Conrey, R.M., 1993. Major and trace element analyses of rocks and minerals by automated X-ray spectrometry. Open file report, Washington State University, Pullman, Washington.

Irvine, T.N., and Baragar, W.R.A., 1971. A guide to the chemical classification of the common volcanic rocks. Canadian Journal of Earth Sciences, **8**, p. 523-548.

Melson, W.G. and Thompson, G., 1971. Petrology of a transform fault zone and adjacent ridge sediments. Philosophical Transactions of the Royal Society of London, **A.268**, p. 423-41.

Meschede, M., 1986. A method of discriminating between different types of mid-ocean ridge basalts and continental tholeiites with the Nb-Zr-Y diagram. Chemical Geology, **56**, p. 207-218.

Miller, C. and Thöni, M., 1995. Origin of eclogites from the Austroalpine Ötztal basement (Tirol, Austria): geochemistry and Sm-Nd vs. Rb-Sr isotope systematics. Chemical Geology, **122**, p. 199-225.

Miyashiro, M.A., 1974. Volcanic rock series in island arcs and active continental margins. American Journal of Science, **274**, p. 321-355.

Miyashiro, M.A., and Shido, F., 1975. Tholeiitic and calc-alkali series in relation to behaviour of Ti, V, Cr, and Ni. American Journal of Science, **275**, p. 265-273.

Mørk, M.B.E. and Mearns, E.W., 1986. Sm-Nd isotopic systematics of a gabbro-eclogite transition. Lithos, **19**, p. 255-267.

Mørk, M.B.E., Kullerud, K. and Stabel, A., 1988. Sm-Nd dating of Seve eclogites, Norrbotten, Sweden - Evidence for early Caledonian (505 Ma) subduction. Contributions to Mineralogy and Petrology, **99**, p. 344-351.

Mortensen, J.K., 1992. Pre-Mesozoic tectonic evolution of the Yukon-Tanana Terrane, Yukon and Alaska. Tectonics, **11**, p. 836-853.

Mortensen, J.K. and Jilson, G.A., 1985. Evolution of the Yukon-Tanana terrane evidence from southeastern Yukon Territory. Geology, **13**, p. 806-810.

Paquette, J.-L., Ménot, R.-P. and Peucat, J.-J., 1989. REE, Sm-Nd and U-Pb zircon study of eclogites from the Alpine External Massifs (Western Alps): evidence for crustal contamination. Earth and Planetary Science Letters, **96**, p. 181-198.

Pearce, J.A., 1982. Trace element characteristics of lavas from destructive plate boundaries. *in* Andesites: Orogenic Andesites and Related Rocks. edited by R.S. Thorpe, John Wiley and Sons, New York, p. 525-548.

Pearce, J.A., 1983. Role of the sub-continental lithosphere in magma genesis and continental margins. *in* Continental Basalts and Mantle Xenoliths. edited by C.J. Hawkesworth and M.J. Norry, Shiva, Cambridge, MA., p. 230-249

Pearce, J.A. and Cann, J.R. 1973. Tectonic setting of basaltic rocks determined using trace element data. Earth and Planetary Science Letters, **19**, p. 290-300.

Pearce, J.A., and Norry, M.J., 1979. Petrographic implications of Ti, Zr, Y and Nb variations in volcanic rocks. Contributions to Mineralogy and Petrology, **69**, p. 33-47.

Pearce, J.A.and Parkinson, I.J., 1993. Trace element models for mantle melting: Application to volcanic arc petrogenesis. *in* Magmatic Processes and Plate Tectonics. edited by H.M. Pritchard et al., Geological Society Special Publication, **76**, p. 373-403.

Pearce, J.A., Baker, P.E., Harvey, P.K. and Luff, I.W., 1995. Geochemical evidence for subduction fluxes, mantle melting and fractional crystallization beneath the South Sandwich Island arc. Journal of Petrology, **36**, p. 1073-1109.

Roback, R.C., Sevigny, J.H. and Walker, N.W., 1994. Tectonic setting of the Slide Mountain terrane, southern British Columbia. Tectonics, **13**, p. 1242-1258.

Sanders, I.S., van Calsteren, P.W.C. and Hawkesworth, C.J., 1984. A Grenville Sm-Nd age for the Glenelg eclogite in north-west Scotland. Nature, **312**, p. 439-440.

Shervais, J.W., 1983. Ti/V plots and the petrogenesis of modern and ophiolitic lavas. Earth and Planetary Science Letters, **59**, p. 101-108.

Smith, A.D. and Lambert, R. St.J., 1995. Nd, Sr and Pb isotope evidence for contrasting origins of Late Paleozoic volcanic rocks from the Slide Mountain and Cache Creek terranes, south-central British Columbia. Canadian Journal of Earth Sciences, **32**, p. 447-459.

Stevens, R.A., 1994. Structural and tectonic evolution of the Teslin tectonic zone, Yukon: a doubly vergent transpressive shear zone. Unpublished Ph.D. thesis, University of Alberta, 130 pp.

Stevens, R.A. and Erdmer, P., 1996. Structural divergence and transpression in the Teslin Tectonic zone, southern Yukon Territory. Tectonics, **15**, p. 1342-1363.

Stevens, R.A., Erdmer, P., Creaser, R.A. and Grant, S.L., 1996. Mississippian assembly of the Nisutlin assemblage: evidence from primary contact relationships and Mississippian magmatism in the Teslin Tectonic Zone, part of the Yukon-Tanana Terrane of south-central Yukon. Canadian Journal of Earth Sciences, **33**, p. 103-116.

Tempelman-Kluit, D.J., 1976. The Yukon Crystalline Terrane: enigma in the Canadian Cordillera. Geological Society of America Bulletin, **87**, p. 1343-1357.

Tempelman-Kluit, D.J., 1979. Transported cataclasite, ophiolite, and granodiorite in Yukon: evidence of a arc-continent collision. Geological Survey of Canada, **Paper 79-1A**, p. 1-12.

Thöni, M. and Jagoutz, E., 1992. Some new aspects of dating eclogites in orogenic belts: Sm-Nd, Rb-Sr and Pb-Pb isotopic results from the Austroalpine Saualpe and Koraalpe type-locality (Carinthia/Styria, southeastern). Geochimica et Cosmochimica Acta, **56**, p. 347-368.

Vidal, P. and Hunziker, J.C., 1985. Systematics and problems in isotope work on eclogites. Chemical Geology, **52**, p. 129-141.

Wanless, R.K., Stevens, R.D., Lachance, G.R. and Delabio, R.N., 1978. Age determinations and geological studies: K-Ar isotopic ages, report 13. Geological Survey of Canada, **Paper 77-2**, 60 pp .

Wasserburg, G.J., Jacobsen, S.B., DePaolo, D.J., McCulloch, M.T. and Wen, T., 1981. Precise determinations of Sm/Nd ratios, Sm and Nd isotopic abundances in standard solutions. Geochimica et Cosmochimica Acta, **45**, p. 2311-2323.

Wheeler, J.O., Brookfield, A.J., Gabrielse, H., Monger, J.W.H., Tipper, H.W. and Woodsworth, G.J., compilers, 1988. Terrane Map of the Canadian Cordillera. Geological Survey of Canada, Open File, **1894**.

Wheeler, J.O. and McFeely, P., compilers, 1987. Tectonic assemblage map of the Canadian Cordillera and adjacent parts of the United States of America. Geological Survey of Canada, Open File **1894**.

Wheeler, J.O. and McFeely, P., compilers, 1991. Tectonic assemblage map of the Canadian Cordillera and adjacent parts of the United States of America. Geological Survey of Canada, **map 1712A**, scale 1:2,000,000.

Winchester, J.A., and Floyd, P.A., 1977. Geochemical discrimination of different magma series and their differentiation products using immobile elements. Chemical Geology, **20**, p. 325-343

Appendix 1: Analytical Methods

Seventeen whole rock eclogite samples and ten garnet and clinopyroxene mineral separates were analyzed for their geochemical signatures. Major and trace elements were determined at Washington State University by x-ray fluorescence (XRF) and inductively coupled plasma mass spectrometric (ICPMS) techniques (Hooper et al., 1993). Neodymium analyses were performed at the University of Alberta on a suite of eight whole rock samples and eighteen mineral separates.

Samples were crushed to gravel size without direct contact with any metal surfaces, followed by final grinding in an agate mill to less than 35 microns. Garnet and clinopyroxene separates were prepared using a combination of shaker table, Frantz magnetic separator and heavy liquid techniques.

Sample powders for Sm-Nd isotopic analyses were weighed and totally spiked with a tracer solution of ^{150}Nd and ^{149}Sm. Initially samples were dissolved in a 5:1 mix of vapour distilled 24N HF and 16N HNO_3 in sealed 30 ml teflon vessels at 160° C for ~ 96 hours. The resulting solution was evaporated to dryness, 6N HCl was added to the residue and heated at 160° C for 24 hours to dissolve fluorides. This method of

dissolution was ineffective in the garnet separates as considerable undissolved residue remained and after experimentation the method was modified. A 1:1 mixture of 16N HNO_3 and millipore water was added to the garnet samples in sealed 120 ml teflon vessels and subsequently heated at 150° C for 24 hours. The solution was then cooled, 10 ml 24N HF added and heated at 150° C for ~ 72-96 hours. The resulting solution was evaporated to dryness and 6N HCl added to the residue and heated at 120° C for 24 hours. The same procedure was then followed for each of the samples. The solution was evaporated and the residue was heated in a loading solution of 0.75N HCl for ~ 12 hours prior to separation of the rare earth elements as a group using standard cation chromatography. Nd was separated from Sm using di(2-ethylhexyl phosphate) chromatography (HDEHP).

The purified Nd and Sm fractions were analyzed for isotopic composition using VG 354 and MM 30 mass spectrometers. Both Nd and Sm were loaded on double rhenium filament beads as chlorides. For later analyses, Nd was converted to nitrate prior to loading. Total procedural blanks for Nd and Sm are < 300 pg. The ^{150}Nd-^{149}Sm tracer solution was made from highly purified material; ^{150}Nd = 97.62 at.%, ^{149}Sm = 97.22 at.%. ^{150}Nd and ^{149}Sm concentrations in the solution were determined by direct calibration in

triplicate against a mixed Sm-Nd normal solution (Wasserburg et al., 1981) with reproducibility of better than ± 0.01% for ^{150}Nd and ± 0.03% for ^{149}Sm.

A dynamic multicollector procedure was used for isotopic analysis of Nd, correcting the raw ratios both for variable mass-discrimination to $^{146}Nd/^{144}Nd = 0.7219$ using an exponential law (Wasserburg et al., 1981), and for the effects of low abundance (non-^{150}Nd) tracer Nd isotopes. Sm was analyzed in static multicollector mode and corrections were made both for variable mass-discrimination to $^{152}Sm/^{147}Sm = 1.17537$ using exponential law (Wasserburg et al., 1981), and for the effects of low abundance (non-^{149}Sm) Sm tracer isotopes on $^{152}Sm/^{154}Sm$.